Progress In Electromagnetics Research B, Vol. 89, 87–109, 2020

Theory of Electromagnetic Radiation in Nonlocal Metamaterials — Part II: Applications

Said Mikki*

Abstract—We deploy the general momentum space theory developed in Part I in order to explore nonlocal radiating systems utilizing isotropic spatially-dispersive metamaterials. The frequency-dependent angular radiation power density is derived for both transverse and longitudinal external sources, providing detailed expressions for some special but important cases like time-harmonic- and rectangular-pulse-excited small dipoles embedded into such isotropic metamaterial domains. The fundamental properties of dispersion and radiation functions for some of these domains are developed in examples illustrating the features in nonlocal radiation phenomena, including differences in bandwidth and directivity performance, novel virtual array effects, and others. In particular, we show that by a proper combination of transverse and longitudinal modes, it is possible to attain perfect isotropic radiators in domains excited by small sinusoidal dipoles. The directivity of a nonlocal small antenna is also shown to increase by possibly four times its value in conventional local domains if certain design conditions are met.

1. INTRODUCTION

The principal goal of this paper is to demonstrate how the general momentum-space theory of Part I [1] can be deployed to help understanding the basic radiation properties of elementary sources embedded into such nonlocal metamaterials. Some general issues related to the overall scope of this work and the design of metamaterials for radiating nonlocal systems had already been discussed in the introductory sections of Part I and Sec. 5 there and the reader is referred to that material for further information. In the remaining part of this Introduction, we focus on providing a general overview of the content of the present paper.

We start with Sec. 2, which is dedicated to presenting the main rudimentary facts (supported by the Appendix) about the main genre of nonlocal metamaterials considered in Part II, namely the generic *isotropic* medium whose essential features pertinent to radiation theory are briefly sketched out in Sec. 2.1. After that, we further specialize the general isotropic case in Sec. 2.2 to concentrate for the rest of this paper on the special but substantial example of *non-resonant* isotropic nonlocal metamaterials (NR-NL-MTM). In Sec. 3, we start investigating the first concrete antenna type in this paper, a point source, dipole-like radiator embedded into the NR-NL-MTM described in the previous section. To do so, we first need to slightly modify the previous theory to deal with continuous sources, which necessitates the introduction of the *momentum space power spectral radiation density function* by applying a careful limiting process when the radiation energy test interval T goes to infinity. Starting from Sec. 4, we focus on concrete antenna sources launching longitudinal (L) waves and explore the dispersion data of such radiating systems and estimate the corresponding fundamental momentum-space radiation functions. A specific temporal dispersion profile (generic Drude model) is assumed due

Received 1 May 2020, Accepted 27 July 2020, Scheduled 12 October 2020
* Corresponding author: Said Mikki (said.m.mikki@gmail.com).
The author is with the Zhejiang University/University of Illinois at Urbana-Champaign Institute (ZJU-UIUC) Institute, Haining, Zhejiang, China.

to its popularity and wide applicability and the main features of nonlocality consequent on this choice are investigated. The results of the previous sections are then combined in Sec. 5 to disclose one of the most outstanding features of nonlocal radiating antenna systems, the phenomenon of *virtual arrays* where careful manipulation of the processes of launching multiple T and L modes is found to lead to the presence of an array-factor-like radiation pattern even when only a single physical source is used. The general expressions for this system are derived and some numerical examples are given. The directivity of a combined L-T nonlocal antenna system excited by a small dipole is shown to vary with frequency and mode excitation type, with the possibility of increasing directivity from 1.5 in classical (local) antennas to values as high as 6 (i.e., four-fold increase due to the use of nonlocal MTM domains.) Another remarkable feature of nonlocal radiating systems is the possibility to synthesize a perfectly isotropic radiation pattern, a feature unique to nonlocal MTMs and is shown to depend crucially on the excitation of L modes. We provide an engineering application case study in Sec. 6, where exact MTM design equations were derived for the case of point (dipole) source excitation energized by a sinusoidal signal. We also point out possible generalization to implement approximation of isotropic radiators over a desired frequency range for wideband applications like time-dependent arrays, UWB systems, and nonsinusoidal antennas. Finally, we end with conclusions and recommendations for future work.

2. THE GENERAL THEORY OF ISOTROPIC NONLOCAL METAMATERIALS

2.1. Principal Radiation Formulas in Isotropic Nonlocal Metamaterials

One of the simplest — yet still demanding and interesting — nonlocal media is the special case of isotropic, homogeneous, spatially-dispersive, but optically inactive domains [2]. In this case, very general principles force the generic expression of the material response tensor to acquire the concrete form [3–5]:

$$\boxed{\overline{\overline{\varepsilon}}(\mathbf{k},\omega)=\varepsilon^{\mathrm{T}}(k,\omega)(\bar{\mathbf{I}}-\hat{k}\hat{k})+\varepsilon^{\mathrm{L}}(k,\omega)\hat{k}\hat{k},} \tag{1}$$

where $k := |\mathbf{k}|$, $\hat{k} := \mathbf{k}/k$, and $\mathbf{k}$ is the wavevector (spatial-frequency) of the field. The first term in the RHS of Eq. (1) represents the *transverse* parts of the response function, while the second is the *longitudinal* component, with behaviour captured by the generic functions $\varepsilon^{\mathrm{T}}(k,\omega)$ and $\varepsilon^{\mathrm{L}}(k,\omega)$, respectively. The tensorial forms involving the dyads $\hat{k}\hat{k}$, however, are imposed by the formal requirement of the need to satisfy the Onsager symmetry relations in the absence of external magnetic fields [5]. In Appendix A, we provided detailed further information about several prominent quantities expected to play a key role in the general radiation theory of nonlocal materials. In particular, in order to estimate the antenna radiation pattern using the general formulas [1]

$$U_l(\mathbf{k})=\frac{1}{\varepsilon_0}\mathbf{J}^*_{\mathrm{ant}}[\mathbf{k},\omega_l(\mathbf{k})]\cdot\overline{\mathbf{R}}_l(\mathbf{k})\cdot\mathbf{J}[\mathbf{k},\omega_l(\mathbf{k})],\quad U_l(\mathbf{k})=\frac{1}{\varepsilon_0}R_l(\mathbf{k})\ \mathbf{J}^*_{\mathrm{ant}}[\mathbf{k},\omega_l(\mathbf{k})]\cdot(\overline{\mathbf{I}}-\hat{k}\hat{k})\cdot\mathbf{J}_{\mathrm{ant}}[\mathbf{k},\omega_l(\mathbf{k})], \tag{2}$$

we need to evaluate the fundamental function $R_l(\mathbf{k})$ for several exemplary cases. This is already available through the formula (A10) derived in Appendix A. It is interesting however to note that one may also utilize the alternative general expression [1]

$$R_l(\mathbf{k})=\left.\frac{\omega}{\frac{\partial}{\partial\omega}\left[\omega^2\ \hat{e}^*_l(\mathbf{k})\cdot\overline{\overline{\varepsilon}}^{\mathrm{H}}(\mathbf{k},\omega)\cdot\hat{e}_l(\mathbf{k})\right]}\right|_{\omega=\omega_l(\mathbf{k})} \tag{3}$$

after specializing the material tensor by means of Eq. (1). Both computational methods were found to lead to the same answer. In either case, *what is really at stake is to know the dispersion relations*, at least for the use of (A10), and both the dispersion relation and the modal polarization when formulas like Eq. (3) are used.

The dispersion relation is given by substituting Eq. (A4) into the general equation $G^{-1,\mathrm{H}}(\mathbf{k},\omega)=0$ derived in [1], leading to $\varepsilon^{\mathrm{L}}(k,\omega)\left[\varepsilon^{\mathrm{T}}(k,\omega)-n^2\right]^2=0$, which is readily satisfied provided either the longitudinal (L) or the transverse (T) waves are excited. In details, for the L modes we denote these dispersion data by

$$\varepsilon^{\mathrm{L}}(k,\omega)=0\ \ \Rightarrow\ \ \text{L modes}:\ \omega=\omega^{\mathrm{L}}_l(k),\ \ \hat{e}_l(\mathbf{k})=\hat{k}, \tag{4}$$

where the modal fields are obviously polarized along the wavevector $\mathbf{k}$. Note that such modes do not exist in domains like free space, while if they exist in local temporally dispersive media, e.g., cold plasma waves, they don't effectively couple energy into the radiation zone because without spatial dispersion their group velocity is zero [2]. On the other hand, for T waves, two degenerate modal fields $\hat{e}_{ls}(\mathbf{k})$, $s = 1, 2$, exist and are both contained in the plane perpendicular to $\mathbf{k}$. Their dispersion relations are clearly

$$\varepsilon^{\mathrm{T}}(k,\omega) - n^2 = 0 \;\Rightarrow\; \text{T modes}: \; \omega = \omega_l^{\mathrm{T}}(k), \;\; \hat{e}_{ls}(\mathbf{k}) \cdot \hat{k} = 0, \;\; \hat{e}^*_{ls_1}(\mathbf{k}) \cdot \hat{e}_{ls_2}(\mathbf{k}) = \delta_{s_1 s_2}, \;\; s_{1,2} = 1, 2. \quad (5)$$

Such ls-modes are analogous to classical (local) antenna radiation fields but their behaviour and properties can be very different due to the peculiarity of nonlocal domains as will be seen below in some selected examples below.

We now may directly calculate the radiation spectral structure functions for both modes. For L waves, use of Eqs. (A10) and (4) gives

$$R_l^{\mathrm{L}}(\mathbf{k}) = \left. \frac{1}{\omega \dfrac{\partial \varepsilon^{\mathrm{L}}(k,\omega)}{\partial \omega}} \right|_{\omega = \omega_l^{\mathrm{L}}(k)}, \quad (6)$$

where the L mode dispersion relation $\varepsilon^{\mathrm{L}}\left(k, \omega_l^{\mathrm{L}}(k)\right) = 0$ was used. A similar procedure for the case of T waves yields

$$R_l^{\mathrm{T}}(\mathbf{k}) = \left. \frac{1}{\omega \dfrac{\partial}{\partial \omega}\left[\varepsilon^{\mathrm{T}}(k,\omega) - n^2(k,\omega)\right]} \right|_{\omega = \omega_l^{\mathrm{T}}(k)}, \quad (7)$$

after the use of $\varepsilon^{\mathrm{T}}\left(k, \omega_l^{\mathrm{T}}(k)\right) - n^2(k, \omega_l^{\mathrm{T}}(k)) = 0$, the dispersion relation of T modes. It is interesting to note that the two $R_l(\mathbf{k})$ functions share the same form for both L and T waves even though the underlying dispersion data are quite different. We also notice the complete decoupling between the two types of waves. In general, such neat separation of waves into uncoupled T and L modes is not possible in arbitrary anisotropic domains [5]. Precisely the same formulas (6) and (7) can be obtained if we start with Eq. (3), providing self-consistency of our calculations but the details are omitted.

2.2. Nonresonant Isotropic Nonlocal Metamaterials

For the remainder of this paper, a series of elementary concrete examples will be given in order to illustrate some of the basic features of nonlocal antennas. Let us start with a class of nonlocal metamaterials called *nonresonant nonlocal metamaterial* (NR-NL-MTM) in which the material dielectric functions can be expanded in the power series

$$\varepsilon^{\mathrm{L}}(k,\omega) = \sum_{i=0}^{N} a_i(\omega) k^{2i}, \quad \varepsilon^{\mathrm{T}}(k,\omega) = \sum_{i=0}^{N} b_i(\omega) k^{2i}, \quad (8)$$

where N is some integer terminating the series expansion, the *order* of the MTM.[†] Let us further fix $N = 1$. In this case, the NR-NL-MTM response model in Eq. (8) reduces to

$$\varepsilon^{\mathrm{L}}(k,\omega) = a_0(\omega) + a_1(\omega) k^2, \quad \varepsilon^{\mathrm{T}}(k,\omega) = b_0(\omega) + b_1(\omega) k^2. \quad (9)$$

The L mode dispersion relation in Eq. (4) then becomes $\varepsilon^{\mathrm{L}}(k,\omega) = a_0(\omega) + a_1(\omega) k^2 = 0$, which can be readily solved to give

$$k = \left[\frac{-a_0(\omega)}{a_1(\omega)}\right]^{1/2}. \quad (10)$$

[†] The L and T dielectric functions need not share the same upper bound on the number of terms but we assume so here for simplicity. The form in Eq. (8) often arises in practice, especially for media with no excitation of strong resonant modes like surface waves [2, 4]. Media that may exhibit such behaviour include homogenized arrays with strong near-field mutual coupling between the unit cells [6], materials with weak spatial dispersion [2], and some plasma materials at certain frequency/phase velocity range [7, 8], and numerous others.

Note that we assume $a_0(\omega) > 0$, $a_1(\omega) < 0$, as is expected from the basic underlying physics [2, 3, 9]. Moreover, we also assume the same for the transverse response function, i.e., $b_1(\omega) < 0$, $b_0(\omega) < 0$, which is the case for the same reasons as the L wave response. The negative root was discarded in Eq. (10) because we already expect from symmetry that for every $\mathbf{k}$-wave, the wave associated with $-\mathbf{k}$ is also a solution but not of interest here since we are focusing on radiation away from the source/antenna (The same is done below for T waves.).

The T mode dispersion relation in Eq. (5) gives $b_0(\omega) + b_1(\omega)k^2 - n^2 = 0$, which after using $n^2 = c^2k^2/\omega^2$ simplifies to $\omega^2 b_0(\omega) + \left(\omega^2 b_1(\omega) - c^2\right) k^2 = 0$. The positive root solution of this equation is

$$k = \left[\frac{\omega^2 b_0(\omega)}{(c^2 - \omega^2 b_1(\omega))}\right]^{1/2}, \tag{11}$$

which constitutes the T mode dispersion relation for $N = 1$ (again the negative root is discarded).

Using the alternative form of the dispersion relation written in terms of the refraction index in Eq. (B1), the T wave dispersion law can be found by

$$n_{\mathrm{T}}^2(\omega) = \frac{b_0(\omega)}{c^2 - \omega^2 b_1(\omega)}, \tag{12}$$

where n_{T} is the function only of ω but is independent of $\hat{k}$. When there is no spatial dispersion, $b_1 = 0$ and Eq. (12) reduces to the familiar $n = \sqrt{\varepsilon}$ law in local homogeneous and isotropic domains. Fig. 1 illustrates the T wave dispersion data in the two forms, the index of refraction function in Fig. 1(a), and the direct $k = k(\omega)$ function in Fig. 1(b). We study the T wave propagation characteristics within a given frequency band with center frequency ω_c, which could serve as the carrier frequency in an analog or digital communication system. The strength of spatial dispersion is varied according to the normalized parameter $\zeta := -\omega_c^2 b_1/c^2$, with no spatial dispersion when $\zeta = 0$. As can be seen from both figures, as frequency increases, the propagation characteristics strongly deviates from the local antenna scenario as ζ increases. In particular, the frequency-dependent index of refraction $n_{\mathrm{T}}(\omega)$ appears to asymptotically approach zero when spatial dispersion is very strong. This suggests that nonlocal T wave antennas may experience reduced radiation bandwidth under conditions of strong nonlocality, an observation that will be confirmed by further results below.

To estimate the nonlocal antenna radiation pattern, we need to evaluate the fundamental $R_l(\mathbf{k})$ function. Using Eq. (6) with the L mode dispersion relation in Eqs. (10) and (9), straightforward

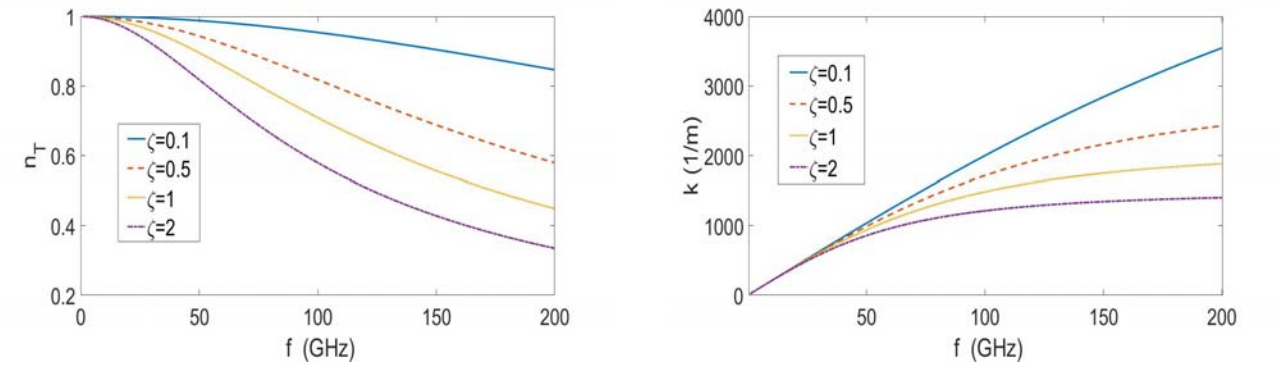

Figure 1. Dispersion analysis results for the nonresonant nonlocal metamaterial (NR-NL-MTM) whose model is given by (8) with case $N = 1$. We also further assume here negligible T wave response temporal dispersion ($b_0 = 1$, $\partial b_1(\omega)/\partial\omega = 0$). (a) The transverse refraction index n_{T} as function of frequency. (b) The transverse (T wave) mode dispersion relation. Here, $\zeta := -\omega_c^2 b_1/c^2$, where $\omega_c := (\omega_{\max} - \omega_{\min})/2$ is the center frequency in the frequency band $[\omega_{\min}, \omega_{\max}]$.

calculations give

$$R_l^{\mathrm{L}}(k) = \left.\frac{1}{\omega\left[a_0'(\omega) + a_1'(\omega)k^2\right]}\right|_{\omega=\omega_l^{\mathrm{L}}(k)}, \tag{13}$$

where $\omega_l^{\mathrm{L}}(k)$ can be obtained by inverting Eq. (10) and the prime indicates differentiation. For the T modes, using Eq. (B1) in Eq. (7), the following expression is obtained for the T wave case:

$$R_l^{\mathrm{T}}(k) = \left.\frac{1}{\omega\dfrac{\partial}{\partial\omega}\varepsilon^{\mathrm{T}}(k,\omega) + 2n^2(k,\omega)}\right|_{\omega=\omega_l^{\mathrm{T}}(k)} = \left.\frac{1}{2n(k,\omega)\dfrac{\partial}{\partial\omega}[\omega n(k,\omega)]}\right|_{\omega=\omega_l^{\mathrm{T}}(k)}, \tag{14}$$

where $\omega_l^{\mathrm{T}}(k)$ is found by inverting Eq. (11). With the help of Eq. (9), expression (14) can be put into the following general form

$$R_l^{\mathrm{T}}(k) = \left.\frac{1}{\omega b_0'(\omega) + \omega b_1'(\omega)k^2 + \dfrac{2c^2 b_0(\omega)}{c^2 - \omega^2 b_1(\omega)}}\right|_{\omega=\omega_l^{\mathrm{T}}(k)}. \tag{15}$$

The expressions (13) and (15) can handle arbitrary temporal dispersion profiles for antennas radiating into isotropic nonlocal media of class $N = 1$ NR-NL-MTM. To gain further insight into the basic behaviour of such antennas, we focus on the special but important case of negligible temporal dispersion.[‡] That is, for simplicity let us further assume that no temporal dispersion exists in the transverse dielectric response case, which is mathematically expressed by

$$b_0(\omega) = 1, \quad b_1'(\omega) = 0. \tag{16}$$

Therefore, the coefficients of the power series expansion in Eq. (8) are not dependent on frequency. For the special case of Eq. (16), the relation in Eq. (15) may be further reduced into

$$R^{\mathrm{T}}(k) = \left.\frac{1}{2n_{\mathrm{T}}^2}\right|_{\omega=\omega_{\mathrm{T}}(k)} = \frac{c^2 - \omega_{\mathrm{T}}^2(k)b_1}{2c^2}, \tag{17}$$

where for simplicity we removed the modal index l since only one T wave exists for $N = 1$.[§] In Sec. 3, the formula (17) will be exploited to explore various properties and characteristics of basic sources embedded into such class $N = 1$ NR-NL-MTM.

3. TRANSVERSE WAVE NONLOCAL ANTENNA SYSTEMS

We are ready now to tackle our first elementary radiating antenna system: the fundamental infinitesimal dipole antenna radiating at single frequency. This is nothing but a very short thin-wire antenna concentrated at a position (say the origin) with orientation $\hat{\alpha}_s$ and frequency ω_s. In spite of its extreme simplicity, this source has received considerable attention in classical antenna theory, usually under the rubric of *Hertizan dipole* [10], or electrically small antennas [11]. Moreover, it can be shown that any current that is not electrically small can be expanded into an optimized infinitesimal dipole model composed of only a few such infinitesimal sources [12–15]. For these reasons, we propose that understanding the basic behaviour of a T wave nonlocal antenna should start with a thorough investigation of such fundamental infinitesimal-dipole-based nonlocal antenna systems. Extension to L wave type and arrays will be given in Secs. 4 and 5, respectively.

[‡] Indeed, even though nonlocal metamaterials are expected to exhibit both spatial and temporal dispersion behaviour, in certain frequency bands and wavenumber ranges, these two types of dispersion can be treated as independent phenomena [2, 3].

[§] It should be remembered that since b_1 is negative, the ratio $R^{\mathrm{T}}(k)$ is always positive and in fact less than one. Similarly, one can show that $R^{\mathrm{L}}(k)$ is between 0 and 1. Such inequalities follow from fairly general energy relations in dispersive electromagnetic media imposed by thermodynamic considerations and are valid also for anisotropic MTMs, e.g., see [3, 9].

3.1. The Momentum Space Radiation Power Pattern of Continuous Sources

The expression of the infinitesimal dipole sinusoidal antenna current in spacetime is given by

$$\mathbf{J}_{\rm ant}(\mathbf{r},t)=\hat{\alpha}_s J_s\delta(\mathbf{r}-\mathbf{r}_s)e^{-{\rm i}\omega_s t},\quad \mathbf{J}_{\rm ant}(\mathbf{k},\omega)=\hat{\alpha}_s e^{{\rm i}\mathbf{k}\cdot\mathbf{r}_s}2\pi J_s\delta(\omega-\omega_s), \tag{18}$$

where $\mathbf{r}_s$ is the location of the source and the frequency-dependent complex-valued quantity $J_s=J_s(\omega_s)$ its strength. In order to utilize the radiation energy density expression [1]

$$U_l(\mathbf{k})=\frac{1}{\varepsilon_0}R_l(\mathbf{k})\left|\hat{k}\times\mathbf{J}_{\rm ant}[\mathbf{k},\omega_l(\mathbf{k})]\right|^2, \tag{19}$$

we evidently need to square a delta function because of Eq. (18). This can be achieved with the help of the generalized function identity [16, 17]

$$[2\pi\delta(\omega-\omega_s)]^2=T2\pi\delta(\omega-\omega_s), \tag{20}$$

where T is the duration of the excitation, and the limit $T\to\infty$ is implicit here. The spherical coordinates form of $\hat{k}$ is given by

$$\hat{k}=\hat{k}(\Omega)=\hat{x}\cos\varphi\sin\theta+\hat{y}\cos\varphi\sin\theta+\hat{z}\cos\theta, \tag{21}$$

where $\Omega:=(\theta,\varphi)$ and ${\rm d}\hat{k}={\rm d}\Omega$. With the help of Eq. (20) after substituting Eq. (18) into Eq. (19), making use of Eqs. (17) and (21), we arrive at

$$P_{\rm T}(k,\hat{k})=\frac{c^2-\omega_{\rm T}^2(k)b_1}{2c^2\varepsilon_0}\left|(\hat{x}\cos\varphi\sin\theta+\hat{y}\cos\varphi\sin\theta+\hat{z}\cos\theta)\times\hat{\alpha}_s\right|^2\,2\pi|J_s|^2\delta(\omega_{{\rm T},k}-\omega_s), \tag{22}$$

where the *momentum-space power spectral density* is defined by

$$\boxed{P_l(\mathbf{k}):=\lim_{T\to\infty}\frac{U_l(\mathbf{k})}{T}.} \tag{23}$$

The expression (22) gives the radiated power per unit momentum-space volume ${\rm d}^3k/(2\pi)^3$ for transverse (T) waves emitted by a point source oriented along $\hat{\alpha}_s$ with source tuned to frequency ω_s. The angles θ and φ are those associated with observation in momentum space, hence their identification with $\hat{k}$. For example, the total power radiated in the angular sector $\Omega_r\ni\hat{k}$ and within the wavenumber range $k_1<k<k_2$ is given by

$$P_{\rm rad}(k_1<k<k_2,\,\hat{k}\in\Omega_r)=\int_{k_1}^{k_2}{\rm d}k\int_{\Omega_r}{\rm d}\Omega\cdot P_{\rm T}(k,\hat{k}). \tag{24}$$

Physically, a radiation function of the form $P(k,\hat{k})$ measures the radiated power density per unit solid angle per unit wavenumber, with units of Watt per solid angle per 1/m.

The wavenumber k can be considered a measure of the inverse of the characteristic wavelength of the field's spatial variation, so for small k the field possesses very large λ-components, while short-wavelength components correspond to $k\to\infty$ [3, 4]. However, in controlled radiation theory, we rarely enjoy fully freedom in regard to manipulating the production of the source's wavelength components. Instead, what is typically available is the *frequency* of the externally-applied source/natural process pumping energy into the nonlocal material/metamaterial.

Now the key idea of this paper is that radiated energy can be computed in both momentum space and spacetime. Note that the delta function in Eq. (22) forces only one T mode to be excited, that in which $\mathbf{k}$ satisfies the condition $\omega(\mathbf{k})=\omega_s$. This corresponds to the familiar condition in local radiation theory where all emitted waves must satisfy $k=\omega_s/c$; however, due to the increased number and complexity of modes associated with radiation into nonlocal media, the antenna radiation pattern is expected to be significantly altered qualitatively and quantitatively as will be discussed in Sec. 5.

Consequently, what is needed next is a general expression for the nonlocal antenna radiation pattern expressed as function of angles and frequency instead of angles and k, i.e., a function of the form $U_l(\omega,\hat{k})$ or $P_l(\hat{k};\omega)$ in line of the proposal given toward the end of Part I. We provide here a simple method to derive such frequency-dependent radiation pattern valid for the case of generic isotropic nonlocal

domains. The most natural method is to equate energy in both representations, i.e., $U_l(\omega,\hat{k})$ is *defined* by the equality:

$$\int \frac{\mathrm{d}^3k}{(2\pi)^3}U_l(\mathbf{k}) = \int \mathrm{d}\omega \int \mathrm{d}\Omega\; U_l(\omega,\hat{k}). \tag{25}$$

Note that in this paper we interchange $\hat{k}$ and Ω whenever convenient, see Eq. (21). To do so, the dispersion relation $\omega_l(\mathbf{k})$ will be used, but in the more appropriate form

$$\mathbf{k}_l(\omega) = k_l(\omega)\hat{k} \tag{26}$$

valid only if the index of refraction $n_l(\omega,\hat{k})$ defined by Eq. (B1) is independent of $\hat{k}$, which *is* the case in *isotropic* nonlocal media (The generalization to arbitrary media is given in Appendix B). The function $k = k_l(\omega)$ is obtained by inverting the dispersion relation $\omega = \omega_l(k)$. Note that by construction there is only one mode captured by the dispersion relation $\omega_l(k)$ so this function is injective (one-to-one), and hence invertible with one k-root for the equation $\omega_l(k) - \omega = 0$, which we denote by k_l.

Now, in spherical coordinates, the volume element in the momentum (spatio-spectral) space $\mathbf{k}$ may be written as $\mathrm{d}^3k = \mathrm{d}kk^2\mathrm{d}\Omega$, while $\mathrm{d}k = (\mathrm{d}k_l/\mathrm{d}\omega)\mathrm{d}\omega$. Therefore, the LHS of Eq. (25) can be expanded as

$$\int \frac{\mathrm{d}^3k}{(2\pi)^3}U_l(\mathbf{k}) = \int \mathrm{d}\omega k^2 \frac{\mathrm{d}k_l(\omega)}{\mathrm{d}\omega} \int \mathrm{d}\Omega U_l[k_l(\omega),\hat{k}]. \tag{27}$$

Comparing Eq. (27) with Eq. (25), it is possible to deduce that

$$\boxed{U_l(\omega,\hat{k}) = \frac{k_l^2(\omega)}{(2\pi)^3}\frac{\mathrm{d}k_l(\omega)}{\mathrm{d}\omega}\,U_l[k_l(\omega),\hat{k}].} \tag{28}$$

Physically, the quantity in Eq. (28) represents *the radiation energy density, or energy per unit solid angle per unit radian frequency* (Watt per starad per rad/s). The total energy radiated within a frequency band $[\omega_1,\omega_2]$ and angular sector Ω_r is given by

$$U_{\mathrm{rad}}(\omega_1 < \omega < \omega_2, \hat{k} \in \Omega_r) = \int_{\omega_1}^{\omega_2} \mathrm{d}\omega \int_{\Omega_r} \mathrm{d}\Omega\, U_l(\omega,\hat{k}). \tag{29}$$

On another hand, it is quite straightforward to compute the radiation pattern in terms of *power* instead of energy. Using Eqs. (28) in (23), the observable radiation power pattern of the nonlocal point source can be put in the form

$$\boxed{P_{\mathrm{T}}(\theta,\varphi;\omega) = \frac{\omega^2}{16\pi^3\varepsilon_0 c^2\sqrt{c^2-\omega^2 b_1}}\,|(\hat{x}\cos\varphi\sin\theta + \hat{y}\cos\varphi\sin\theta + \hat{z}\cos\theta)\times\hat{\alpha}_s|^2\,2\pi|J_s|^2\delta(\omega-\omega_s),} \tag{30}$$

where ω_s is the externally supplied (antenna) source frequency and the T wave dispersion relation in Eq. (11) was utilized. The relation in Eq. (30) constitutes the *T wave antenna (angular) radiation power density* (radiation pattern for short), i.e., the amount of power radiated by the T mode in the direction (θ,φ) per unit frequency when a sinusoidal point source with frequency ω_s and orientation $\hat{\alpha}_s$ excites an isotropic nonresonant nonlocal metamaterial with $N = 1$. In particular, the total radiated power in the solid angular sector $\Omega_r := \{\theta_1 < \theta < \theta_2,\, \varphi_1 < \varphi < \varphi_2\}$ can be computed by means of the formula

$$P_{\mathrm{rad}}(\Omega_r) = \int_0^\infty \mathrm{d}\omega \int_{\Omega_r} \mathrm{d}\Omega P_{\mathrm{T}}(\theta,\varphi;\omega) = \int_0^\infty \mathrm{d}\omega \int_{\theta_1}^{\theta_2}\int_{\varphi_1}^{\varphi_2} \mathrm{d}\theta\mathrm{d}\varphi\sin\theta\; P_{\mathrm{T}}(\theta,\varphi;\omega). \tag{31}$$

The proof of Eq. (31) follows directly from the manner in which U_l was constructed via relations of the form in Eq. (27).

3.2. Antenna Directivity Analysis

Moving further, the sinusoidal radiator *directivity* is defined as *the ratio of the maximum radiated power density divided by the isotropic power density* (the latter being the power density corresponding to ideal isotropic radiator.) Quantitatively, this is given by [11]

$$D(\omega) := \frac{\max_{\theta,\varphi} P(\theta,\varphi;\omega)}{P_{\rm rad}(4\pi;\omega)/2\pi}, \tag{32}$$

where $P_{\rm rad}(4\pi;\omega_s)$ is the radiated power on the entire infinite sphere. To give a concrete example, let us assume that the point antenna is located at the origin and oriented along the z-direction. In this case, $|\hat{k}\times\hat{\alpha}_s| = |\hat{k}\times\hat{z}| = |\sin\theta|$. From Eqs. (30) and (31), it follows that

$$P_{\rm rad}(4\pi;\omega) = \frac{|J_s|^2\omega^2}{8\pi^2\varepsilon_0 c^2\sqrt{c^2-\omega^2 b_1}}\int_0^{2\pi}\mathrm{d}\varphi\int_0^{\pi}\mathrm{d}\theta\sin^3\theta \ = \frac{|J_s|^2\omega^2}{3\pi\varepsilon_0 c^2\sqrt{c^2-\omega^2 b_1}}, \tag{33}$$

where $\int_0^{\pi}\mathrm{d}\theta\sin^3\theta = 4/3$ was used. On the other hand,

$$\max_{\theta,\varphi} P_{\rm T}(\theta,\varphi;\omega) = \frac{|J_s|^2\omega^2}{8\pi^2\varepsilon_0 c^2\sqrt{c^2-\omega^2 b_1}}\max_{\theta,\varphi}|\sin^3\theta| = \frac{|J_s|^2\omega^2}{8\pi^2\varepsilon_0 c^2\sqrt{c^2-\omega^2 b_1}}. \tag{34}$$

Therefore, from Eq. (32), the T wave nonlocal antenna has directivity $D_{\rm T} = 1.5$, which is the same as its value for local infinitesimal antennas. Therefore, sinusoidal T wave antennas of modes described by dispersion relation in Eq. (11) exhibit the same directive properties as conventional free-space antenna.[‖]

In Fig. 2, we illustrate one of those curious divergences in behaviour between local and nonlocal radiators. Fig. 2(a) shows the radiated total power (power radiated by all polarization components in all directions) computed by means of the expression (30) over a frequency band. The case with $\zeta = 0$ corresponds to zero spatial dispersion, i.e., local antennas (free-space radiators.) On the other hand, the cases $\zeta = 0.1, 0.5, 1$, model class $N = 1$ non-resonant in isotropic metamaterials with increasing spatial dispersion strength, respectively. It is clear that the celebrated $1/\lambda^2$ power law in electromagnetic transmission is no longer satisfied at large frequencies in the case of this nonlocal T wave antenna system. Indeed, the local antenna possesses a ω^2 frequency law, while spatially dispersive media with the T wave mode of the class $N = 1$ exhibits a *linear* ω frequency law or $1/\lambda$ variation for high frequency. This implies that electromagnetic waves radiated by this type of nonlocal T modes would experience greater decay of their high-frequency components, leading to smaller transmission bandwidth compared with local antennas. This striking behaviour can also be noticed in Fig. 2(b) where we plot the angular radiation pattern of a point source parallel to the z-direction, so θ measures the angle with the z-axis. It can be seen that with significant spatial dispersion ($\zeta = 1$), the peak radiated power level of the T wave nonlocal antenna class $N = 1$ drops like $1/f$ with increasing frequency relative to the peak level attained by the local antenna at the same frequency range.

3.3. Radiation Energy Patterns for Pulsed Signals

It is interesting to note that the theory developed in this paper is not exclusively restricted to sinusoidal sources of the form in Eq. (18). In fact, the momentum space approach is quite general and can handle arbitrary radiators in both space and time. To give a flavour of this possible expansion of the method, we stay within the relatively simple confines of the class $N = 1$ nonresonant nonlocal metamaterial we have been exploring so far but now assume that the radiating source is excited by a rectangular pulse $\mathrm{rect}(t/T)$, where T is the total pulse duration.[¶] The antenna current distribution in this case can be

[‖] Note, however, that this does *not* imply that directivity is the same in all other cases. The nonlocal antenna remains fundamentally different from conventional free-space antennas in many respects. The first element among these distinctions is the existence of *multiple* modes in nonlocal radiators, e.g., both T and L waves, which inherently changes the radiation pattern, leading to what was described previously as "intrinsic material array effect" emerging from the fact that several modes may act like array antenna even though only a single physical radiator exists [18–21]. Some of these directive emission differences marking nonlocal and local antenna systems are elaborated in general and for a few examples in Sec. 5.

[¶] See Fig. 3(b). Such pulses are essential in studying and designing modern digital communications. For example, digital data streams can be modeled as a series of shifted rectangular pulses [22], see Fig. 3(a).

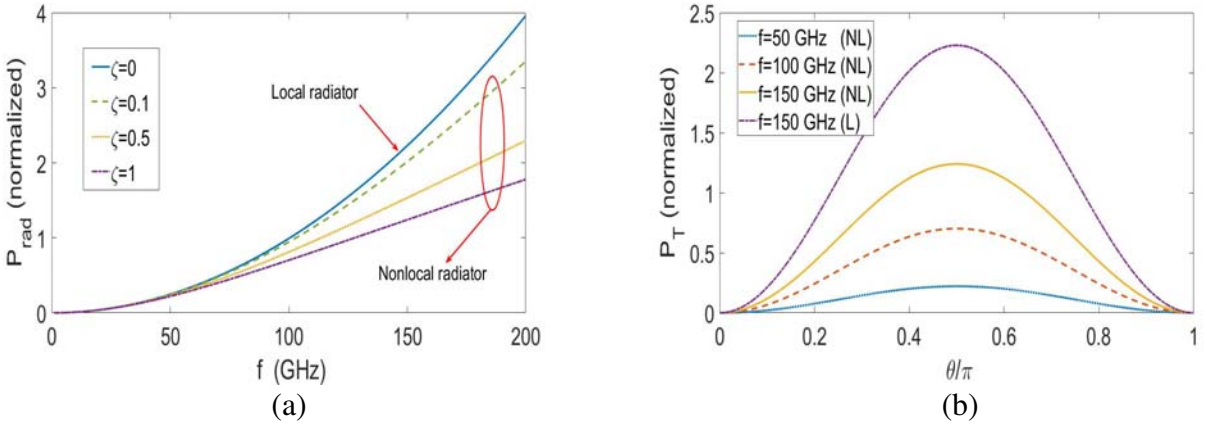

Figure 2. T wave radiated power density pattern results for a sinusoidal radiator embedded into the nonresonant nonlocal metamaterial (NL-MTM) given by Eq. (8) with $N = 1$. We also further assume here negligible temporal dispersion ($b_0 = 1$, $\partial b_1(\omega)/\partial\omega = 0$). The normalized radiated power is defined as $P_{\rm rad}/(3\pi\varepsilon_0 c^3 w_c^2)^{-1}$. (a) The radiated power as function of frequency computed using Eq. (30). Here, $\zeta := -\omega_c^2 b_1/c^2$, where $\omega_c := (\omega_{\max} - \omega_{\min})/2$ is the center frequency in the frequency band $[\omega_{\min}, \omega_{\max}]$. (b) Total power radiated by a point source oriented along the z-direction. All results on the nonlocal (NL) antennas are computed for the case of $\zeta = 1$. The local antenna (L) case is clearly $\zeta = 0$, while all other cases refer to nonlocal (NL) antennas (The L used in this figure should not be confused with longitudinal waves used everywhere else in this paper.).

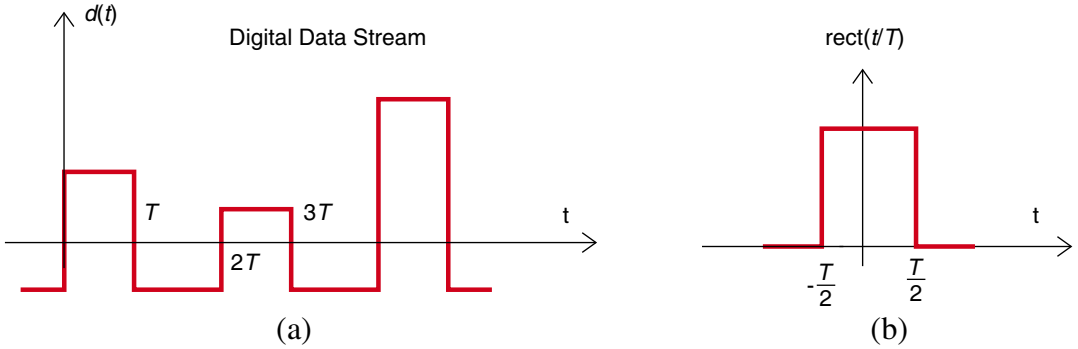

Figure 3. Rectangular pulses carry information in a digital communications link, e.g., (a) a digital data stream signal $d(t)$. (b) A typical rectangular pulse is shown and is used to excite a point dipole source embedded into a nonlocal metamaterials to explore the impact of such engineered domains on electromagnetic radiation for potential deployment in wireless communications.

expressed in spacetime and momentum space via the relations

$$\mathbf{J}_{\rm ant}(\mathbf{r},t) = \hat{\alpha}_s J_s \delta(\mathbf{r}-\mathbf{r}_s)\,{\rm rect}(t/T), \quad \mathbf{J}_{\rm ant}(\mathbf{k},\omega) = \hat{\alpha}_s J_s T\, e^{i\mathbf{k}\cdot\mathbf{r}_s}{\rm sinc}\left(\frac{\omega T}{2}\right), \tag{35}$$

respectively, where $\hat{\alpha}_s$, J_s, and T are the source parameters and ${\rm sinc}(x) := \sin(\pi x)/\pi x$ is the sinc function. Substituting Eqs. (19), (35) and (17) into Eq. (28), the radiation energy density $U_l(\Omega;\omega)$ can be obtained, and after taking the limit in Eq. (23) we arrive at the momentum space radiation energy density

$$U_{\rm T}(\theta,\varphi;\omega) = \frac{J_s^2 T^2 \omega^2 |{\rm sinc}(\omega T/2)|^2}{16\pi^3\varepsilon_0 c^2\sqrt{c^2-\omega^2 b_1}}\left|(\hat{x}\cos\varphi\sin\theta + \hat{y}\cos\varphi\sin\theta + \hat{z}\cos\theta)\times\hat{\alpha}_s\right|^2, \tag{36}$$

where the dispersion relation in Eq. (11) was used. Similar to the calculation in Eq. (33), the total energy radiated by a dipole with rectangular pulse excitation can be obtained and is found to be given

by

$$U_{\rm rad}(\omega)=\frac{|J_s|^2T^2\omega^2|{\rm sinc}(\omega T/2)|^2}{6\pi^2\varepsilon_0c^2\sqrt{c^2-\omega^2b_1}}. \tag{37}$$

This is the positive (single-sided) power spectral density. To compute the net energy radiated by the rectangular pulse, we integrate over all frequencies:

$$\mathcal{E}_{\rm rad}=2\int_0^\infty {\rm d}\omega P_{\rm rad}(\omega)=\int_0^\infty {\rm d}\omega\frac{|J_s|^2T^2\omega^2|{\rm sinc}(\omega T/2)|^2}{3\pi^2\varepsilon_0c^2\sqrt{c^2-\omega^2b_1}}. \tag{38}$$

Figure 4 shows some results based on the expressions (36) and (37) for an infinitesimal dipole oriented along the z-direction. We apply a rectangular pulse with width $T=\gamma 2\pi/\omega_c$, where ω_c is the center frequency of the frequency-band sweep. The degree of spatial dispersion is measured as before using the parameter ζ with the local antenna corresponding to $\zeta=0$. In Fig. 4(a), the radiation energy function for a dipole's rectangular pulse excitation width of $T=2\pi/\omega_c$ is plotted against frequency for the case of local MTM ($\zeta=0$) and three scenarios of successive cases of nonlocal antennas experiencing increase in spatial dispersion ($\zeta=0.1,0.5,1$). As we can see, the local antenna case exhibits very strong second resonance peak at 150 GHz following the main resonance at 50 GHz. However, for nonlocal antennas, the second resonance is significantly attenuated in comparison with the free-space antenna. This is consistent with the results we saw previously in Fig. 2(b) where it was noticed that the nonlocal T wave antenna's radiation density of single mode exhibits weaker frequency growth compared with local antennas. Here, the actual computation of the antenna's radiation energy in Fig. 4(a) clearly confirms the reduction in radiation bandwidth suspected in Fig. 1 with the analysis there of the corresponding basic modal dispersion law.

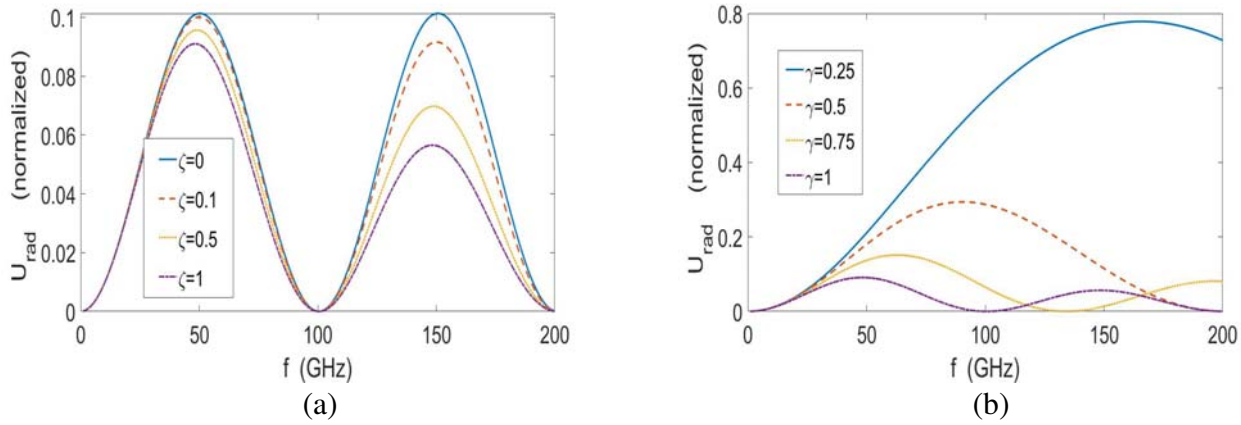

Figure 4. T wave radiated energy results for a pulsed-excited point source oriented along the z-direction embedded into the nonresonant nonlocal metamaterial (NR-NL-MTM) given by Eq. (8) with $N=1$ and negligible temporal dispersion ($b_0=1$, $\partial b_1(\omega)/\partial\omega=0$)). The antenna is excited by a rectangular pulse with duration T as in Fig. 3. The normalized radiated energy is $U_{\rm rad}/(J_s^2T^2/3\pi\varepsilon_0c^3w_c^2)^{-1}$ where $\omega_c:=(\omega_{\max}-\omega_{\min})/2$ is the center frequency in the frequency band $[\omega_{\min},\omega_{\max}]$. (a) Radiated energy as function of frequency for $\zeta=-\omega_c^2b_1/c^2$ and $T=2\pi/w_c$. (b) Study of the impact of the excitation pulse width $T=\gamma 2\pi/\omega_c$ on the T wave nonlocal antenna's radiated energy with T wave spatial dispersion strength parameter $\zeta=1$.

On the other hand, Fig. 4(b) illustrates the impact of the excitation window pulse duration on the radiation density. The energizing pulse width T is varied according to $2\pi\gamma/\omega_c$ with $\gamma=0$, successively assuming increasing values $0.25,0.5,0.75,1.0$ (these results are obtained for nonlocal MTM $\zeta=1$.) As expected, when the pulse width increases, less frequency components become available to excite transverse modes and the overall excitation approaches a DC or constant signal when $T\to\infty$, which explains why radiation dampens with increasing T.[+]

[+] We also add that the decay of the energy spectral density $U_{\rm rad}(\omega)$ shown in Fig. 4(b) is very weak, making the convergence of

4. LONGITUDINAL WAVE NONLOCAL ANTENNA SYSTEMS

Longitudinal (L) waves represent the second major type of electromagnetic waves excitable by sources embedded into nonlocal domains. The corresponding radiating systems will be dubbed L *wave nonlocal antennas.*[♯] Our goal here is to investigate when such waves can be excited and how the combined T wave response developed in Sec. 3 and L wave radiation (to be developed shortly in this section) can be joined together (the L-T array effect to be discussed in Sec. 5).

4.1. Some General Considerations for L Waves

Let us begin by first pointing out a peculiar fact about longitudinal waves. Since for L modes the wave is polarized along the direction of propagation, we have $\hat{e}_l^*(\mathbf{k}) = \hat{k}$, and therefore the L wave momentum-space radiation energy density derived in Part I can be put in the form

$$U_l(\mathbf{k}) = \frac{1}{\varepsilon_0} R_l(\mathbf{k}) |\hat{k} \cdot \mathbf{J}_{\text{ant}}[\mathbf{k}, \omega_l(\mathbf{k})]|^2. \tag{39}$$

Writing the equation of continuity in the spatio-temporal domain then converting it to the momentum space, we obtain, respectively

$$\frac{\partial \rho_{\text{ant}}(\mathbf{r}, t)}{\partial t} + \nabla \cdot \mathbf{J}_{\text{ant}}(\mathbf{r}, t) = 0, \quad \mathbf{k} \cdot \mathbf{J}_{\text{ant}}(\mathbf{k}, \omega) = \omega \rho_{\text{ant}}(\mathbf{k}, \omega), \tag{40}$$

where ρ_{ant} is the electric charge density of electrical source corresponding to the externally applied current distribution $\mathbf{J}_{\text{ant}}$. Substituting Eq. (40) into Eq. (39), the following general form is obtained

$$U_l(\mathbf{k}) = \frac{R_l(k) \omega_l^2(\mathbf{k})}{k^2 \varepsilon_0} |\rho_{\text{ant}}(\mathbf{k}, \omega)|^2. \tag{41}$$

The expression (41) is as good as the original form in Eq. (39). However, in certain applications, such as microscopic emission processes and certain applications in nanotechnology, it might be easier to express the radiating source as a charge density than as an antenna current distribution, and in the latter case the relation in Eq. (41) is clearly more appropriate to work with. Nevertheless, in antenna applications and macroscopic electromagnetics, the formula (39) expressing radiation in terms of surface or volume current distributions is preferred because the geometrical shape of the antenna can often be invoked to restrict the mathematical form of the current.[⋆]

One observation that immediately comes out after examining the L modes radiation formula when expressed in the alternative form Eq. (41) is that such waves can radiate only if the mode frequency $\omega_l(\mathbf{k})$ is nonzero. While this might be expected, note that from the L mode dispersion relation in Eq. (4) the dielectric function $\varepsilon^{\text{L}}(\mathbf{k}, \omega)$ *must* depend on frequency. Otherwise, the equation $\varepsilon^{\text{L}}(\mathbf{k}, \omega) = 0$ will not yield any specific value for ω for a given input $\mathbf{k}$. This is clearer from the special case in Eq. (10), where it is evident that no actual dispersion relation in the form $\omega = \omega_l(k)$ might obtain if the condition $(\partial/\partial\omega)\varepsilon^{\text{L}} \neq 0$ is not satisfied. Therefore, the following conclusions is inevitable: *In contrast to T wave nonlocal radiators, effective L wave radiation would* not *be possible if the L dielectric function ε^{L} is independent of frequency ω.* In other words, unlike T wave sources discussed in Sec. 3, *temporal dispersion is fundamental in order to excite L waves in nonlocal domains.* Therefore, in all the coming calculations we will need to assume some concrete temporal dispersion model for the coefficients $a_i(\omega)$ appearing in (8). However, it is important to remember that longitudinal and transverse response functions are *independent physical processes* in general [2, 4].[&]

the total energy integral (38) slow. This is expected since the rectangular pulse excitation shown in Fig. 3 and implemented in the source function in Eq. (35) assumes zero rise-/fall-times. In other words, this type of excitation current does not possess a first-order derivative, which explains the slow decay of the energy spectral density. However, this represents no problem in principle for our comparative study with nonlocal radiators since both the local and nonlocal antennas are utilizing the same time pulse excitation form. In practice, we replace the ideal rectangular pulse by smooth pulses, e.g., Gaussian pulses [23], and those are known to have Fourier spectra with very rapid frequency decay, e.g., see [17].

[♯] In Sec. 2.2, the dispersion relation of L waves launched into isotropic media were derived, see the general Equation (4), and the special case of class $N = 1$ non-resonant type metamaterial in Eq. (10).

[⋆] For example, in one dimensional antennas like wires or loops, the direction of current flow is fixed once and for all by the geometry. In cases like these and numerous others, the evaluation of the radiation energy density $U_l(\mathbf{k})$ is expected to be considerably easier using Eq. (39) than Eq. (41).

[&] That is, while in some problems they may get entangled with each other, fundamentally speaking the dielectric functions ε^{L} and

4.2. The Radiation Power Pattern of L Wave Antenna Systems

To evaluate the L wave radiation density function, it is to be noted first that the density expression (28) is still valid for L waves and hence when combined with Eq. (39) would give

$$U_{\mathrm{L}}(\omega,\hat{k})=\frac{k_{\mathrm{L}}^2(\omega)}{\varepsilon_0(2\pi)^3}\frac{\mathrm{d}k_{\mathrm{L}}(\omega)}{\mathrm{d}\omega}\,R^{\mathrm{L}}(\omega)|\hat{k}\cdot\mathbf{J}_{\mathrm{ant}}[k_{\mathrm{L}}(\omega),\hat{k}]|^2 \tag{42}$$

as the radiation energy pattern for the L wave antenna. Here, $R^{\mathrm{L}}(\omega):=R[k_{\mathrm{L}}(\omega)]$.[^] Substituting the L mode dispersion relation in Eq. (10) into Eq. (13) gives

$$R_{\mathrm{L}}(\omega)=\frac{1}{\omega\left[a_0'(\omega)+a_1'(\omega)\dfrac{a_0(\omega)}{-a_1(\omega)}\right]}=\frac{a_1(\omega)/\omega}{a_0'(\omega)a_1(\omega)-a_1'(\omega)a_0(\omega)}. \tag{43}$$

Furthermore, from Eq. (6) we have

$$\frac{\mathrm{d}k_{\mathrm{L}}(\omega)}{\mathrm{d}\omega}=\frac{1}{2k_{\mathrm{L}}}\frac{\mathrm{d}}{\mathrm{d}\omega}\left[\frac{a_0(\omega)}{-a_1(\omega)}\right]=\frac{-1}{2k_{\mathrm{L}}}\frac{a_0'(\omega)a_1(\omega)-a_1'(\omega)a_0(\omega)}{a_1^2(\omega)}. \tag{44}$$

Consequently, Eq. (42) evaluates to

$$U_{\mathrm{L}}(\hat{k};\omega)=\frac{-n_{\mathrm{L}}(\omega)}{2\varepsilon_0c(2\pi)^3a_1(\omega)}\left|\hat{k}\cdot\mathbf{J}_{\mathrm{ant}}[k_{\mathrm{L}}(\omega),\hat{k}]\right|^2, \tag{45}$$

where the L wave index of refraction n_{L} is given by

$$n_{\mathrm{L}}(\omega):=\frac{k_{\mathrm{L}}(\omega)c}{\omega}=\frac{c}{\omega}\sqrt{\frac{a_0(\omega)}{-a_1(\omega)}} \tag{46}$$

It is not possible to proceed further without specifying the functional forms of $a_0(\omega)$ and $a_1(\omega)$. As stated earlier, these are some of the main MTM design parameters available for the material engineer. For maximum clarity and concreteness, let us assume that this design data is given by

$$a_0(\omega)=1-\frac{\omega_p^2}{\omega^2},\quad -a_1(\omega)=\frac{g^2}{\omega^2}, \tag{47}$$

which means that the host domain dielectric response function $a_0(\omega)$ is assumed to follow the classical Drude model with Plasma frequency ω_p. The parameter g is assumed to be a positive real number. Its value, together with ω_p, may be determined by the material's physics and design. The dispersion relation of the L wave in Eq. (10) now takes the form

$$k_{\mathrm{L}}^2(\omega)=\frac{1}{g^2}\left(\omega^2-\omega_p^2\right),\quad \omega_{\mathrm{L}}^2(k)=\omega_p^2+g^2k^2. \tag{48}$$

It is interesting to observe that the choice $g=\sqrt{3}V_e$, where V_e is the thermal electron velocity in a hot plasma, results in the famous dispersion relation of Langmuir waves [2, 7]. Here, the thermal velocity is equal to $\sqrt{k_{\mathrm{B}}T_e/m_e}$, where T_e and m_e are the temperature of the electron gas and the electron mass, respectively, while k_{B} is Boltzmann constant. While the underlying physical realization of nonlocal metamaterials need not be restricted to plasma structures, we mention in passing that the Langmuir-type dispersion relations obtained with the choice $g=\sqrt{3}V_e$ are often considered accurate when the phase velocity $v_p=\omega/k$ is large compared with the thermal velocities of all species in the thermal plasma.[≀] In general, the L mode index of refraction in Eq. (46) under the special case in Eq. (48) reduces into

$$n_{\mathrm{L}}(\omega)=\frac{c}{\omega g}\sqrt{\omega^2-\omega_p^2}=\frac{c}{g}\sqrt{1-\frac{\omega_p^2}{\omega^2}}=\frac{c}{g}\,a_0(\omega). \tag{49}$$

ε^{T} can be treated as two distinct functions. The material designer may then try to optimize the performance of some applications by independently controlling the various internal parameters associated with each response function type, i.e., the array functions $a_i(\omega)$ and $b_i(\omega)$.

[^] Note that we specify the L mode dispersion law by the subscript/superscript and suppress the modal index since the $N=1$ class has only one mode but the same formula is valid for other L modes in higher-order classes.

[≀] Usually ionic species are much slower than electrons due to the small electron/nucleus mass ratio provided the various ion gases temperatures are not very large.

Note that for very large frequencies $\omega \gg \omega_p$, $n_{\rm L}(\omega) \sim c/g$, i.e., the index of refraction eventually converges to constant level with increasing frequency, a behaviour very different from the T wave index of refraction $n_{\rm T}(\omega)$ studied earlier, where in the latter case $n_{\rm T}(\omega) \to 0$ as $\omega \to \infty$ for the case of nonlocal media, see Fig. 2(a).

We many now proceed to compute the L wave antenna radiation pattern. Using Eqs. (47) and (49) in Eq. (45) leads to

$$U_{\rm L}(\hat{k};\omega) = \frac{\omega\sqrt{\omega^2-\omega_p^2}}{2\varepsilon_0(2\pi)^3 g^3}\left|\hat{k}\cdot\mathbf{J}_{\rm ant}[k_{\rm L}(\omega),\hat{k}]\right|^2. \tag{50}$$

This is the general L wave radiation formula in our special MTM case. For a sinusoidal antenna with radiating current in Eq. (18), the radiation power density can be obtained by a procedure identical to the one employed to find Eq. (30). The result is

$$\boxed{P_{\rm L}(\theta,\varphi;\omega) = \frac{\omega\sqrt{\omega^2-\omega_p^2}}{16\varepsilon_0\pi^3 g^3}|(\hat{x}\cos\varphi\sin\theta+\hat{y}\cos\varphi\sin\theta+\hat{z}\cos\theta)\cdot\hat{\alpha}_s|^2\ 2\pi J_s^2\delta(\omega-\omega_s).} \tag{51}$$

It is interesting to compare this form of the L mode radiation power density with the corresponding formula for T waves, i.e., Equation (30). Both seem to share several structural features, e.g., similar ω^2 law for large frequencies. Also, since g has the unit of velocity, the appearance of factors containing g^3 in the denominator of the multiplicative fraction of (51) makes the latter very symmetrical in comparison with (30) where g is played there by c. In fact, when we consider the L-T combined response of nonlocal antenna systems in Secs. 5 and 6, it will be found that the ratio between these two characteristic L and T type speeds, namely g/c, will play a fundamental role.

Finally, we add another notable difference between T and L waves. It turns out that the momentum space radiation function $R^{\rm L}(k)$ has a fixed value

$$R^{\rm L}(k) = \frac{1}{2} \tag{52}$$

for L waves. On another hand, the corresponding relation for T waves in Eq. (17) is very different, exhibiting a strong function of k. Equation (52) can be proved by plugging the choice in Eq. (47) into Eq. (43) and performing some additional but straightforward manipulations which are omitted here for brevity.

5. VIRTUAL ARRAYS IN NONLOCAL ANTENNA SYSTEMS

5.1. Principal Formulas

As will be shown below, it turns out that the key to understanding one of the most outstanding features of nonlocal antennas is the existence of *multiple* modes, transverse and longitudinal, that could be excited *simultaneously*, leading to novel and unexpected radiation characteristics of external sources embedded into nonlocal domains. To see this, we continue working with the nonresonant nonlocal metamaterial model given in Eq. (8). The L mode dispersion relation for arbitrary N is obtained from (4) and it assumes the form

$$\sum_{i=0}^{N} a_i(\omega)k^{2i} = 0, \tag{53}$$

which is a polynomial equation in k^2 of order N with frequency-dependent coefficients $b_i(\omega)$. Note that these coefficients are real since by construction the dispersion relation is applied to the *hermitian* part of the response function [1]. However, even with real coefficients, the polynomial equation (53) have N generally complex roots $k_{L,l}$, $l = 1, 2, ..., N$. We are interested only in modes propagating away from the source carrying effective energy to the far zone, so roots with non-negligible imaginary part are discarded and only those solutions of (53) consisting mainly of real wavenumber k are admitted. Let

the number of these by $N_{\mathrm{L}} \leq N$. Similarly, the T wave dispersion relation in Eq. (5) together with Eq. (8) results in the following general polynomial equation in k

$$b_0(\omega) + \left[b_1(\omega) - \frac{c^2}{\omega^2}\right] k^2 + \sum_{i=2}^{N} b_i(\omega) k^{2i} = 0, \tag{54}$$

which is also an N-order polynomial equation in k^2, leading to N generally complex roots $k_{T,l}$, $l = 1, 2, ..., N$. Again, we only admit those roots with positive real part and negligibly small imaginary part. Let us denoted their number by $N_{\mathrm{T}} \leq N$. In sum, a total of $N_{\mathrm{T}} + N_{\mathrm{L}}$ distinct L and T modes may be excited by a nonlocal antenna compatible with a given source excitation frequency ω. Not all waves must be present at the same time and it is expected that a great care must be exhibited to ensure that all modes are actually launched by the externally-introduced current $\mathbf{J}_{\mathrm{ant}}$. In case this situation can be achieved, the total antenna radiation density pattern may be written in the following quite general form

$$U(\omega, \hat{k}) = U^{\mathrm{T}}(\omega, \hat{k}) + U^{\mathrm{L}}(\omega, \hat{k}), \tag{55}$$

where

$$U^{\mathrm{T}}(\omega, \hat{k}) := \sum_{l=1}^{N_{\mathrm{T}}} U_l^{\mathrm{T}}(\omega, \hat{k}) = \sum_{l=1}^{N_{\mathrm{T}}} \frac{k_{\mathrm{T},l}^2(\omega)}{\varepsilon_0 (2\pi)^3} \frac{\mathrm{d}k_{\mathrm{T},l}(\omega)}{\mathrm{d}\omega} R_{\mathrm{T},l}(\omega) |\hat{k} \times \mathbf{J}_{\mathrm{ant}}[k_{\mathrm{T},l}(\omega), \hat{k}]|^2, \tag{56}$$

$$U^{\mathrm{L}}(\omega, \hat{k}) := \sum_{l=1}^{N_{\mathrm{L}}} U_l^{\mathrm{L}}(\omega, \hat{k}) = \sum_{l=1}^{N_{\mathrm{L}}} \frac{k_{\mathrm{L},l}^2(\omega)}{\varepsilon_0 (2\pi)^3} \frac{\mathrm{d}k_{\mathrm{L},l}(\omega)}{\mathrm{d}\omega} R_{\mathrm{L},l}(\omega) |\hat{k} \cdot \mathbf{J}_{\mathrm{ant}}[k_{\mathrm{L},l}(\omega), \hat{k}]|^2. \tag{57}$$

where

$$R_{\mathrm{T},l}(\omega) := R_l^{\mathrm{T}}[k_{\mathrm{T},l}(\omega)], \quad R_{\mathrm{L},l}(\omega) := R_l^{\mathrm{L}}[k_{\mathrm{L},l}(\omega)]. \tag{58}$$

That is, the radiation pattern will consist of two major parts, one generated by all T modes and is given by $U^{\mathrm{T}}(\omega, \hat{k})$, while the L wave contribution is captured by the term $U^{\mathrm{L}}(\omega, \hat{k})$. The data needed to compute the radiation pattern in its most general form are summarized in Table 1. It is to be observed that the momentum-space radiation functions $R_l^{\mathrm{L}}(k)$ and $R_l^{\mathrm{T}}(k)$ can be evaluated via Eqs. (6) and (7), respectively, and that involves only knowledge of both the dielectric functions $\varepsilon^{\mathrm{L}}(\omega, k)$ and $\varepsilon^{\mathrm{T}}(\omega, k)$ and the corresponding dispersion laws.[▷]

Table 1. Data needed to compute the radiation pattern of a generic antenna embedded into an isotropic nonlocal metamaterials with N_{T} and N_{L} T and L modes, respectively, radiating into the far zone.

Data	Description
$\mathbf{J}_{\mathrm{ant}}(\omega, \mathbf{k})$	Momentum-space source current distribution
$k = k_{\mathrm{T},l}(\omega)$, $l = 1, ..., N_{\mathrm{T}}$	N_{T} dispersion functions for the T modes
$k = k_{\mathrm{L},l}(\omega)$, $l = 1, ..., N_{\mathrm{L}}$	N_{L} dispersion functions for the L modes
$\varepsilon^{\mathrm{T}}(\omega, k)$	T wave dielectric function
$\varepsilon^{\mathrm{L}}(\omega, k)$	L wave dielectric function

[▷] From the computational viewpoint, if the dispersion profiles of the modes are available, the only potential difficulty in computing the total radiation pattern would stem from the need to estimate the derivatives $\mathrm{d}k_l/\mathrm{d}\omega$ for every mode. In addition, as can be seen from Eqs. (6) and (7), the calculations of $R_l^{\mathrm{L}}(k)$ and $R_l^{\mathrm{T}}(k)$ themselves require estimating derivatives of the form $\partial\varepsilon/\partial\omega$. In this paper, since all the examples given involve analytical approximation of the dispersion law, this does not present a problem. However, in future work, dispersion analysis of more complicated materials will involve working mainly with numerical data. In that case more careful methods to estimate the group velocity $\mathrm{d}\omega/\mathrm{d}k$ might be required since numerical differentiation is not a stable computational method.

5.2. Virtual Arrays in with Single Sinusoidal Dipole Excitation

In order to better understand the key formulas (56) and (57), let us evaluate them for the special but fundamental case of a point source with sinusoidal excitation as described in Eq. (18). The relevant quantities in this case are the radiation power density obtained by means of Eq. (23) and are given by

$$\boxed{P^{\mathrm{T}}(\omega;\theta,\varphi)=\sum_{l=1}^{N_{\mathrm{T}}}\frac{k_{\mathrm{T},l}^2(\omega)R_{\mathrm{T},l}(\omega)}{\varepsilon_0(2\pi)^3}\frac{\mathrm{d}k_{\mathrm{T},l}(\omega)}{\mathrm{d}\omega}\left|(\hat{x}\cos\varphi\sin\theta+\hat{y}\cos\varphi\sin\theta+\hat{z}\cos\theta)\times\hat{\alpha}_s\right|^2 2\pi J_s^2\delta(\omega-\omega_s)} \tag{59}$$

for the radiation component mediated by T all excited transverse waves, while the corresponding contribution due to longitudinal waves is collected in

$$\boxed{P^{\mathrm{L}}(\omega;\theta,\varphi)=\sum_{l=1}^{N_{\mathrm{L}}}\frac{k_{\mathrm{L},l}^2(\omega)R_{\mathrm{L},l}(\omega)}{\varepsilon_0(2\pi)^3}\frac{\mathrm{d}k_{\mathrm{L},l}(\omega)}{\mathrm{d}\omega}\left|(\hat{x}\cos\varphi\sin\theta+\hat{y}\cos\varphi\sin\theta+\hat{z}\cos\theta)\cdot\hat{\alpha}_s\right|^2 2\pi J_s^2\delta(\omega-\omega_s).} \tag{60}$$

We may now illustrate more directly the *virtual array* effect alluded to above, which is unique to radiation phenomena in nonlocal metamaterials. If one selects the orientation of the radiating dipole to coincide with $\hat{z}$, then the radiation spectral power densities in Eqs. (59) and (60) after integrating over all frequencies ω will result in

$$P_{\mathrm{rad}}^{\mathrm{T}}(\omega_s;\theta,\varphi)\;=\;\frac{J_s^2}{4\varepsilon_0\pi^2}\sum_{l=1}^{N_{\mathrm{T}}}\left.\frac{\mathrm{d}k_{\mathrm{T},l}(\omega)}{\mathrm{d}\omega}\right|_{\omega=\omega_s}k_{\mathrm{T},l}^2(\omega_s)R_{\mathrm{T},l}(\omega)\sin^2\theta, \tag{61}$$

$$P_{\mathrm{rad}}^{\mathrm{L}}(\omega_s;\theta,\varphi)\;=\;\frac{J_s^2}{4\varepsilon_0\pi^2}\sum_{l=1}^{N_{\mathrm{L}}}\left.\frac{\mathrm{d}k_{\mathrm{L},l}(\omega)}{\mathrm{d}\omega}\right|_{\omega=\omega_s}k_{\mathrm{L},l}^2(\omega_s)R_{\mathrm{L},l}(\omega)\cos^2\theta. \tag{62}$$

The expressions (61) and (62) provide radiation patterns *complementary* to each other. We first note that for each T and L radiation law type, the *angular* pattern function, while possessing a temporal frequency ω dependence, is essentially the same, namely that associated with the classic dipole $\sin^2\theta$ law in the case of T waves, and the $\cos^2\theta$ for power law carried by L modes.[◇] On the other hand, if we *combine* the T and L wave radiation patterns in Eqs. (61) and (62) according to Eq. (55), this would result in different phenomena more akin to the *array factor* in conventional (local) antenna theory. Indeed, in this case the total radiated power pattern

$$P_{\mathrm{rad}}(\omega_s;\theta,\varphi)=P_{\mathrm{rad}}^{\mathrm{T}}(\omega_s;\theta,\varphi)+P_{\mathrm{rad}}^{\mathrm{L}}(\omega_s;\theta,\varphi) \tag{63}$$

can be put in the form

$$P_{\mathrm{rad}}(\omega;\theta,\varphi)=\frac{J_s^2A_{\mathrm{L}}(\omega)}{4\varepsilon_0\pi^2}\left[\cos^2\theta+A(\omega)\sin^2\theta\right], \tag{64}$$

where

$$A_{\mathrm{L}}(\omega):=\frac{J_s^2}{4\varepsilon_0\pi^2}\sum_{l=1}^{N_{\mathrm{L}}}\frac{\mathrm{d}k_{\mathrm{L},l}(\omega)}{\mathrm{d}\omega}k_{\mathrm{L},l}^2(\omega)R_{\mathrm{L},l}(\omega),\quad A_{\mathrm{T}}(\omega):=\frac{J_s^2}{4\varepsilon_0\pi^2}\sum_{l=1}^{N_{\mathrm{T}}}\frac{\mathrm{d}k_{\mathrm{T},l}(\omega)}{\mathrm{d}\omega}k_{\mathrm{T},l}^2(\omega)R_{\mathrm{T},l}(\omega), \tag{65}$$

represent the L and T wave complex power pattern amplitudes, respectively, while their all-important T-L power ratio is defined by

$$\boxed{A(\omega):=\frac{A_{\mathrm{T}}(\omega)}{A_{\mathrm{L}}(\omega)}=\frac{\displaystyle\sum_{l=1}^{N_{\mathrm{T}}}\frac{\mathrm{d}k_{\mathrm{T},l}(\omega)}{\mathrm{d}\omega}k_{\mathrm{T},l}^2(\omega)R_{\mathrm{T},l}(\omega)}{\displaystyle\sum_{l=1}^{N_{\mathrm{L}}}\frac{\mathrm{d}k_{\mathrm{L},l}(\omega)}{\mathrm{d}\omega}k_{\mathrm{L},l}^2(\omega)R_{\mathrm{L},l}(\omega)}.} \tag{66}$$

[◇] This, however, is valid for the present special case, and it depends on the radiation source, so the conclusion is not general enough to cover arbitrary nonsinusoidal antennas.

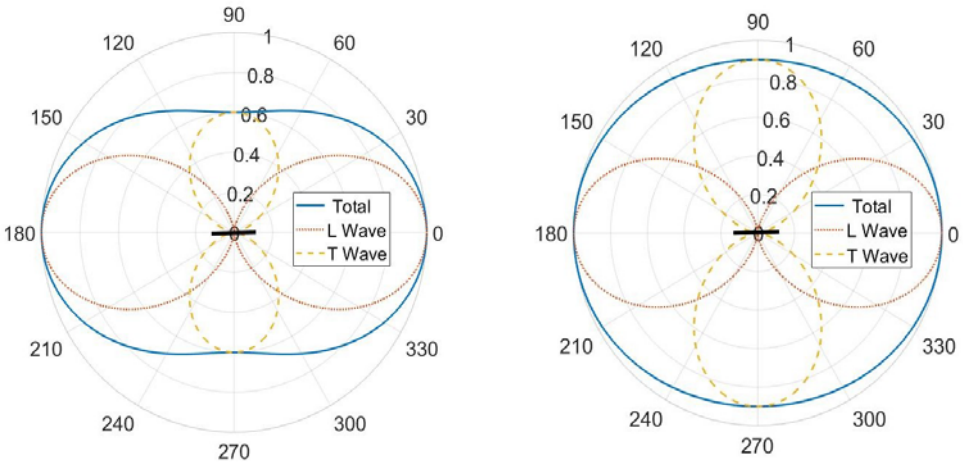

Figure 5. Radiation pattern for a short dipole source oriented along the z-direction and embedded into the isotropic nonresonant nonlocal metamaterial (NR-NL-MTM) described by (8) with class $N = 1$ and negligible T-wave temporal dispersion ($b_0 = 1$, $\partial b_1(\omega)/\partial\omega = 0$). The antenna is excited by a sinusoidal point source with frequency $\omega = 1.1\omega_p$ where ω_p is the plasma frequency for the Drude model of $a_0(\omega)$ given by (47). Only a single L and T modes each are excited here. (a) $A = 0.6$, (b) $A = 0.9$.

The frequency-dependent factors $A_{\rm T}(\omega)$ and $A_{\rm L}(\omega)$ represent the degree of excitation (amplitude and phase) of the transverse- and longitudinal-mediated radiation as can be inferred from Eqs. (61) and (62), respectively.[††] They do not affect the angular radiation pattern of these types of radiation if each was radiated individually. On the other hand, while the common factor $A_{\rm L}(\omega)$ in Eq. (64) still does not affect the angular radiation pattern — exactly as it was in the *individual* T and L mode pattern expressions (61) and (62) — the situation is completely different when we examine the combined T-L pattern . In the latter, it is apparent that the actual radiation angular function *does* depend on the source frequency ω through the complex function $A(\omega)$. When $A = 0$, we recover the pure L mode radiation pattern, while in the other extreme case of $A = \infty$ the entire radiation is transverse. Remarkably, in the special case of $A = 1$, we obtain essentially an *isotropic* radiation pattern though the antenna is oriented along a particular direction (the z-direction in this case.) For values other than 0 and 1, $A(\omega)$ acts like a variable factor shaping the actually attained radiation pattern. As a matter of fact, $A(\omega)$ plays a role similar to *array factor* in conventional antenna theory. The main difference though is that in traditional array theory, the radiated fields are always transverse and the array factor has a simple algebraic form. In nonlocal antenna, however, the T-L mode array factor in Eq. (66) possesses a complicated form ultimately dependent on the material response functions and the dispersion relations. Moreover, in nonlocal antennas the radiated fields are both longitudinal and transverse. In the case represented by Eq. (64), it appears that for sinusoidal point sources the shaping effect due to the nonlocal domain is essentially due to the presence of longitudinal modes.[‡‡]

In Fig. 5, the radiation patterns for two T-L combined array cases are shown where two scenarios are illustrated, with one in which the T-L power ratio is $A = 0.6$ — Fig. 5(a) — and the other is when $A = 0.9$ — Fig. 5(b). The orientation of the dipole is also shown in the figure. *It is evident that dipoles can radiate power along the length of the source, in direct contrast to local (conventional) antennas and this happens because of the excitation of L waves.* Moreover, in the case of nearly equal L and T wave radiation power, the overall radiation pattern approaches a perfectly isotropic radiator form as is seen in Fig. 5(b). The exact case of perfect isotopic radiation occurs when $A = 1$, which will be discussed in details in Sec. 6.

[††] Note that to simplify notation, we replaced ω_s by ω in (64), (65), (66).

[‡‡] This, however, needs not be the case in other, more complex nonlocal antenna systems whose investigation is outside the scope of the present paper. For example, the author expects that complex current sources supporting only T or L waves may deviate from the small dipole type radiation law of T or L waves, respectively, depending on how complex is the spatial distribution of the current throughout the antenna surface. Such more complex radiators include patch-like antennas and will be explored somewhere else.

5.3. Basic Examples

To illustrate the dependence on specific material parameters and frequency, we give a few basic examples based on the $N = 1$ class of isotropic nonresonant nonlocal metamaterial discussed above. From the dispersion relations of the T and L modes with $N_{\rm T} = N_{\rm L} = 1$, i.e., Equations (10) and (11), we readily compute

$$A_{\rm L}(\omega) = \frac{\omega\sqrt{\omega^2 - \omega_p^2}}{8\pi^2\varepsilon_0 g^3}, \quad A_{\rm T}(\omega) = \frac{\omega^2}{8\pi^2\varepsilon_0 c^2\sqrt{c^2 - \omega^2 b_1}}, \quad A(\omega) = \frac{(g/c)^3}{\sqrt{\left(1 - \omega^2 b_1/c^2\right)\left(1 - \omega_p^2/\omega^2\right)}}. \quad (67)$$

Figures 6(a) and 6(b) illustrate the variations of $A(\omega)$ with frequency for several degrees of nonlocality in the T wave response as measured by the normalized parameter ζ. We first observe that as we change ζ from no transverse spatial dispersion ($\zeta = 0$) to stronger transverse nonlocality characterized by larger positive values, the change in the shape of the ratio of power divided between the T and L waves, i.e., the array factor $A(\omega)$, is not very significant. In general, the overall trend observed is strong decline in the T-L power ratio as the operating frequency moves away from the plasma frequency ω_p. This indicates that in this category of nonlocal antenna systems utilizing the $N = 1$-class NR-NL-MTM, power tends to concentrate in the longitudinal wave radiation component with all MTMs behaving as

$$\lim_{\omega\to\infty} A(\omega) = \begin{cases} \frac{g^3}{c^3}, & b_1 = 0, \\ 0, & b_1 \neq 0. \end{cases} \quad (68)$$

In other words, for this class of NR-NL-MTM, the cube of the velocity ratio g/c presents the *minimum* T-L power ratio at very large frequencies, providing a level at which the relative T and L waves' contribution to the total far-field radiation tend to stabilize. As we have seen before, g has the units of speed. If the NL-MTM is to be implemented using plasma domains, then g is likely to reflect the thermal velocity of the charged particles composing the plasma medium, e.g., electrons. In general, we prefer to keep the discussion at a more abstract and generic level in this paper where the goal is to understand the basic physics and design principles of nonlocal radiating systems. No concrete plasma model will be invoked in what follows, but we classify the range of possible values of the g-parameter to three distinctive cases: (i) Nonrelativistic regime ($g \ll c$), (ii) superluminal[11] regime ($g > c$), and (iii) relativistic regime (all remaining values of g). From Eq. (68), we can see that in the nonrelativistic regime, the T-L power ratio is small even when ζ is large (strong T wave response), implying that the L wave contribution to the far field will tend to dominate even when the T wave response is significant. Moreover, at higher frequencies the T-L ratio becomes even considerably smaller since $(g/c)^3$ is much less than $g/c \ll 1$. This case is illustrated in Fig. 6(a). On the other hand, Fig. 6(b) shows that for larger g/c, the T-L power ratio A becomes significantly larger at all frequencies. This suggests that NL-MTMs designed to operate in the relativistic regime exhibit larger contribution of T waves to the far zone. Finally, in the superluminal regimes, calculations show that the T-L ratio could become greater than unity at all frequencies. For $g \to c$ but still $g < c$, $A(\omega)$ may become greater than unity in the lower edge of the frequency range $\omega > \omega_p$.

5.4. Virtual Arrays and Antenna Directivity

Finally, let us estimate the directivity of the nonlocal antenna system exhibiting virtual array effects by focusing on the radiation power pattern in Eq. (64) with the data in Eq. (67). From the definition of directivity formula (32), we have

$$D(\omega) := \frac{\max_{\theta,\varphi} P_{\rm rad(\theta,\varphi;\omega)}}{P_{\rm rad}(4\pi;\omega)/4\pi} = 4\pi\frac{\max_{\theta,\varphi}\left[\cos^2\theta + A(\omega)\sin^2\theta\right]}{\displaystyle\int_0^{2\pi}\mathrm{d}\varphi\int_0^{\pi}\mathrm{d}\theta\sin\theta\left[\cos^2\theta + A(\omega)\sin^2\theta\right]}. \quad (69)$$

[11] The term 'superluminal' does not imply a violation of special relativity since all relevant velocities are *phase* velocities or ω/k, which can be greater than speed of light. Group velocity is usually bounded by the speed of light if expresses energy transport velocity.

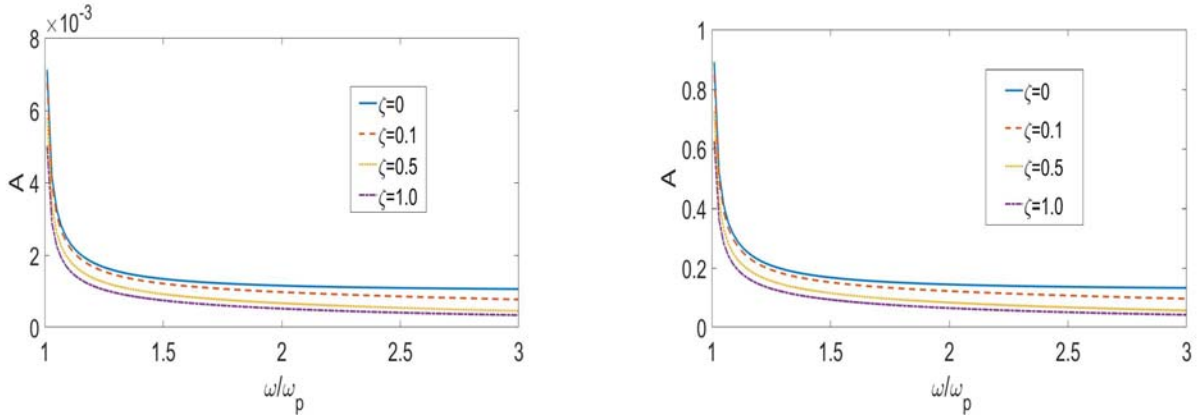

Figure 6. Virtual array effects in the radiation by a point source oriented along the z-direction embedded into class $N = 1$ isotropic nonresonant nonlocal metamaterial (NR-NL-MTM) given by (8) and negligible T wave temporal dispersion ($b_0 = 1$, $\partial b_1(\omega)/\partial\omega = 0$)). The antenna is excited by a sinusoidal point source with frequency ω while ω_p is the plasma frequency for the Drude model $a_0 = 1 - \omega_p^2/\omega^2$ and $a_1 = -g^2/\omega^2$. (a) Variation of $A(\omega)$ with frequency for $g/c = 0.1$. (b) Variation of $A(\omega)$ with frequency for $g/c = 0.5$.

Using $\int_0^\pi \mathrm{d}\theta \sin^3\theta = 4/3$ and $\int_0^\pi \mathrm{d}\theta \sin\theta\cos^2\theta = 2/3$, this evaluates into

$$D(\omega) = \frac{\max_{\theta,\varphi}\left\{1 + [A(\omega) - 1]\sin^2\theta\right\}}{1/3 + 2/3A(\omega)} = \begin{cases} \dfrac{3A(\omega)}{1 + 2A(\omega)}, & A(\omega) \geq 1, \\ \dfrac{6 - 3A(\omega)}{1 + 2A(\omega)}, & A(\omega) < 1. \end{cases} \tag{70}$$

Evidently, this is very different from the classic dipole directivity of $D = 3/2$. In fact, the later is obtained only when $A \to \infty$ since this is the case when $A_\mathrm{L} = 0$, i.e., the L wave does not exist. On the other hand, the maximum directivity that can be attained by this system is $D = 6$ and occurs when $A = 0$, i.e., when the entire radiation is due to L waves. For other intermediate case, the directivity can assume the range of values depicted in Fig. 7. In the range $0 \leq A < 1$, L waves dominate the composition of the radiated fields, while at $A = 1$ the critical transition from L-mode-dominated to T-mode-dominated composition occurs. As A increases, the radiation field tends to become essentially transverse. *Therefore, use of carefully-designed* nonlocal MTMs may lead to significant increase in the directivity of an infinitesimal dipole antenna from 1.5 to 6, i.e., four times the classical antenna directivity.

6. ENGINEERING APPLICATION: SHAPING THE RADIATION PATTERN TO PRODUCE ISOTROPIC ANTENNA SYSTEMS

6.1. Exact Design Equations

A quick application is developed here where the main idea is to theoretically demonstrate how the design of a suitable nonlocal MTM may lead to the construction of future radiating system exhibiting isotropic radiation pattern. For simplicity, we continue to focus on the special but fundamental case of infinitesimal dipole source with time-harmonic excitation. The nonlocal T-L array factor in Eq. (66) can be put in the form

$$A(\omega) = F\left[\omega, \varepsilon^\mathrm{T}(k,\omega), \varepsilon^\mathrm{L}(k,\omega), N_\mathrm{T}, N_\mathrm{L}\right] \tag{71}$$

in order to emphasize the design parameters available to the engineer, where F is the generic functional form of the dependence on such parameters. The data that must be found to design the system are

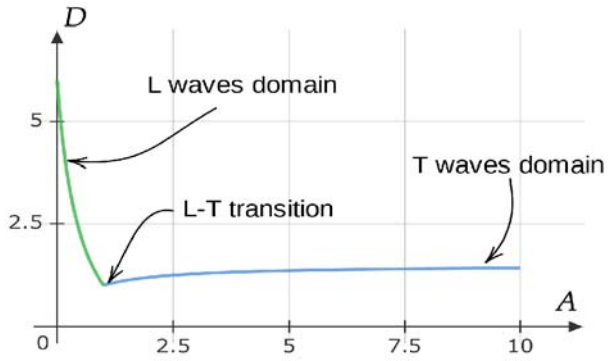

Figure 7. Directiviy of a nonlocal antenna system with single T and L modes vs. the T/L power ratio A.

encoded in the T and L dielectric response functions $\varepsilon^{\mathrm{T}}(k,\omega), \varepsilon^{\mathrm{L}}(k,\omega)$. These in turns determine the dispersion law data $k_{\mathrm{T}}(\omega), k_{\mathrm{L}}(\omega)$. The numbers of T and L modes $N_{\mathrm{T}}, N_{\mathrm{L}}$ must also be determined by the designer. If the desired radiation pattern is required to be isotropic, then from Eq. (64) we easily deduce that a sufficient condition for this to happen is given by the equation $A(\omega) = 1$, or in details

$$\boxed{\sum_{l=1}^{N_{\mathrm{T}}} \frac{\mathrm{d}k_{\mathrm{T},l}(\omega)}{\mathrm{d}\omega}\, k_{\mathrm{T},l}^2(\omega) R_{\mathrm{T},l}(\omega) = \sum_{l=1}^{N_{\mathrm{L}}} \frac{\mathrm{d}k_{\mathrm{L},l}(\omega)}{\mathrm{d}\omega}\, k_{\mathrm{L},l}^2(\omega) R_{\mathrm{L},l}(\omega).} \tag{72}$$

From the form of Eq. (71), the unknowns to be estimated in this case are $\varepsilon^{\mathrm{T}}(k,\omega), \varepsilon^{\mathrm{L}}(k,\omega)$ for a given frequency ω and numbers of modes $N_{\mathrm{T}}, N_{\mathrm{L}}$. The relation in Eq. (72) is the general design equation for sinusoidal isotropic nonlocal antenna systems utilizing an isotropic metamaterial.

We give an example illustrating the design process by specializing for the class $N = 1$ NR-NL-MTM. Making use of Eq. (65), the isotropic radiator design equation (72) reduces to

$$g = c\left[\left(1 - \frac{\omega^2 b_1}{c^2}\right)\left(1 - \frac{\omega_p^2}{\omega^2}\right)\right]^{1/6}. \tag{73}$$

The relation in Eq. (73) represents the main design equation for isotropic nonlocal antenna systems using class $N = 1$ NL-MTM. It spells out the exact connection between this MTM's design parameters b_1 and g on one hand, and the operating frequency on another. Design curves are given in Fig. 8(a) and Fig. 8(b). In Fig. 8(a), the velocity ratio g/c is plotted across frequency for several possible values of ζ, allowing us to assess the impact of the T wave's degree of nonlocality — as measured by ζ — on the ability to attain perfectly isotropic radiators. The results suggest that for local T wave response ($\zeta = 0$), the optimum value of g approaches the speed of light c as the antenna frequency increases sufficiently away from the plasma frequency ω_p since in such scenario we inherently enter the relativistic regime. Hence, to properly design a plasma-type NL-MTM for this application, one needs to operate as close to ω_p as possible if it is desired to remain within the nonrelativistic regime. However, as we start to inject nonlocal behaviour into the MTM by gradually increasing ζ, the optimum value of g shifts into the relativistic regime at much lower frequencies compared with the local T wave case ($\zeta = 0$). In fact, at sufficiently large values for ζ, the optimum g-parameter value enters the superluminal regime at operating frequencies fairly close to ω_p. This general behaviour is further investigated in Fig. 8(b) where we focus on how the optimum value of g changes with the T wave's nonlocality parameter ζ at specific frequency. We there find that whenever the operating frequency is shifted away from ω_p, the NL-MTM design parameters enter the relativistic then the superluminal regimes with even increasing ζ. This behaviour becomes more acute at higher frequencies. For example, in the case of $\omega = 1.5\omega_p$, the

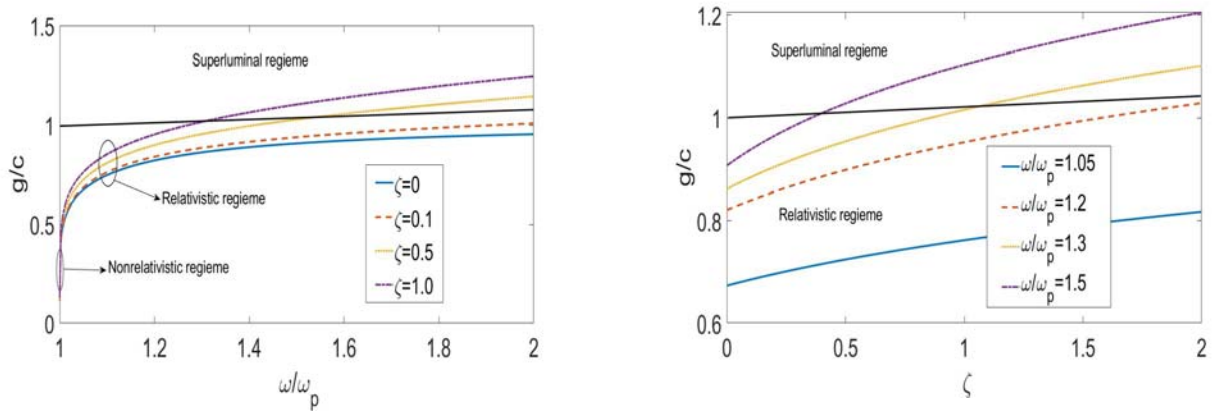

Figure 8. Design curves for perfectly isotropic power radiation by a point source oriented along the z-direction embedded into class $N = 1$ isotropic nonresonant nonlocal metamaterial (NR-NL-MTM) given in (8) and negligible T wave temporal dispersion ($b_0 = 1$, $\partial b_1(\omega)/\partial\omega = 0$)). The antenna is excited by the sinusoidal point source with frequency ω while ω_p is the plasma frequency for the Drude model $a_0 = 1 - \omega_p^2/\omega^2$ and $a_1 = -g^2/\omega^2$. We use (73) to estimate the optimum design value of g in two cases: (a) Variation of optimum isotropic g with frequency for various values of $\zeta := -\omega_p^2 b_1/c^2$. (b) Variation of optimum isotropic g with ζ for various frequencies.

NL-MTM becomes superluminal starting from just around $\zeta = 0.4$. The overall conclusion here is that one would expect the MTM to exhibit weaker T-wave-type nonlocality in order to realize the optimum L wave design parameter g if the latter is to be associated with particle velocities much lower than c.[§§]

6.2. Alternative Design Procedure Based on Optimization

There are two potential difficulties with the exact design equation (72). First, it is not immediately clear that for a given frequency and number of modes that relation can yield useful solution for $\varepsilon^{\mathrm{T}}(k,\omega), \varepsilon^{\mathrm{L}}(k,\omega)$. Even if such solutions exist, the realization of the nonlocal metamaterial might be not available for the range of values obtained. Second, the design approach encapsulated by Eq. (72) is inherently a single-frequency approach and hence inherently narrowband. For many applications, especially modern wireless communication system, the bandwidth could be much larger. To resolve these two difficulties, an approximation is more suited. The idea is that instead of enforcing an *exact* isotropic radiator, one may construct a suitable cost function to measure the deviation of the actually obtained radiation pattern from a target isotropic reference

$$P_{\mathrm{ref}}(\omega;\theta,\varphi) := \frac{J_s^2 A_{\mathrm{L}}(\omega)}{4\varepsilon_0\pi^2}. \tag{74}$$

One such suitable cost measure can be the minimum mean square error (MMSE) function

$$C\left[\varepsilon^{\mathrm{T}}(k,\omega),\varepsilon^{\mathrm{L}}(k,\omega),N_{\mathrm{T}},N_{\mathrm{L}}\right] := \frac{1}{\omega_{\max}-\omega_{\min}}\int_{\omega_{\min}}^{\omega_{\max}} \mathrm{d}\omega \frac{1}{\Omega_r}\int_{\Omega_r} \mathrm{d}\Omega |P_{\mathrm{rad}}(\omega;\theta,\varphi) - P_{\mathrm{ref}}(\omega;\theta,\varphi)|^2, \tag{75}$$

where a convenient numerical optimization of this error will be performed over both the frequency interval of interest $[\omega_{\min},\omega_{\max}]$ and the radiation pattern observed over a given solid angle sector Ω_r. The goal then is clearly to use powerful optimization algorithm to numerically search for the best nonlocal metamaterial parameters $\varepsilon^{\mathrm{T}}(k,\omega), \varepsilon^{\mathrm{L}}(k,\omega), N_{\mathrm{T}}, N_{\mathrm{L}}$, such that the error C is minimum. This is

[§§] However, note that relativistic corrections on speed in plasma have been known long time ago, e.g., see the analysis of the so-called relativistic plasma [2, 4, 8]. Also, radiation phenomena in which the radiating particles are relativistic (Cherenkov radiation) are well understood [4, 24]. Finally, we add that the generic nonresonant nonlocal metamaterial discussed here need not be exclusively realized as hot plasma domain; other technologies might be deployed in the future to implement such metamaterial system such as near-field coupled dense packing domains, metasurfaces, or other periodic structures.

usually attained with additional constraints on the available ranges for these optimization parameters caused by material availability, leading effectively to constrained optimization problems. In this way, a nonlocal metamaterial may be designed to realize a wideband isotropic nonlocal antenna system.

7. CONCLUSION

We provided a detailed application of the general momentum-space radiation theory expounded in Part I focusing on the special but essential case of nonlocal isotropic metamaterials. The specialized dispersion and radiation formulas corresponding to this scenario were derived in details and several analytical and numerical examples were provided to illustrate the use of the theory in describing and designing nonlocal antenna systems. In particular, we studied the behaviour of transverse (T) and longitudinal (L) wave antennas and explored some of their properties. Comparison with local antenna counterparts were given for the cases of time-harmonic and rectangular pulse excitation of infinitesimal dipole sources. Bandwidth and directivity performance were investigated and the distinctive differences between local and nonlocal antennas were explicated. As a more striking difference we also explored virtual array phenomena in nonlocal domains and showed that single sources can have array-factor like radiation pattern. One of the possible engineering applications demonstrated here was the design of perfectly isotropic antenna systems using small dipoles launching a proper combination of T and L waves. Also, we computed the directivity of a combined L-T system and predicted that it may reach four times the value of classical (local) antenna under certain (design) conditions.

APPENDIX A. ISOTROPIC SPATIALLY-DISPERSIVE TENSOR FORMULAS AND SOME OF THEIR PROPERTIES

We work with a medium possessing a dielectric tensor given by Eq. (1). In this case, we can write

$$\overline{\mathbf{G}}^{-1,\,\mathrm{L}}(\mathbf{k},\omega) = \varepsilon^{\mathrm{L}}(k,\omega)\hat{k}\hat{k}, \quad \overline{\mathbf{G}}^{-1,\,\mathrm{T}}(\mathbf{k},\omega) = \left(\varepsilon^{\mathrm{T}}(k,\omega) - n^2\right)(\overline{\mathbf{I}} - \hat{k}\hat{k}), \tag{A1}$$

where the momentum-space dyadic GF

$$\overline{\mathbf{G}}^{-1}(\mathbf{k},\omega) := -\frac{k^2c^2}{\omega^2}\left(\overline{\mathbf{I}} - \hat{k}\hat{k}\right) + \overline{\overline{\varepsilon}}(\mathbf{k},\omega) \tag{A2}$$

from [1] and $n^2 = \frac{k^2c^2}{\omega^2}$ were used. From the definition of matrix determinant, we conclude

$$G^{-1,\mathrm{L}}(\mathbf{k},\omega) = \varepsilon^{\mathrm{L}}(k,\omega), \quad G^{-1,\mathrm{T}}(\mathbf{k},\omega) = \varepsilon^{\mathrm{T}}(k,\omega) - n^2. \tag{A3}$$

It can also be shown by direct calculations that the following decomposition hold

$$G^{-1}(\mathbf{k},\omega) = \varepsilon^{\mathrm{L}}(k,\omega)\left[\varepsilon^{\mathrm{T}}(k,\omega) - n^2\right]^2. \tag{A4}$$

On the other hand, expanding the co-factor matrix into longitudinal and transverse parts, we arrive at

$$\overline{\mathbf{C}}(\mathbf{k},\omega) = \left(\varepsilon^{\mathrm{T}}(k,\omega) - n^2\right)\left[\left(\varepsilon^{\mathrm{T}}(k,\omega) - n^2\right)\hat{k}\hat{k} + \varepsilon^{\mathrm{L}}(k,\omega)(\overline{\mathbf{I}} - \hat{k}\hat{k})\right]. \tag{A5}$$

In particular, the forward Green's function of this special nonlocal medium acquires the simple form

$$\overline{\mathbf{G}}(\mathbf{k},\omega) = \frac{\left(\varepsilon^{\mathrm{T}}(k,\omega) - n^2\right)\hat{k}\hat{k} + \varepsilon^{\mathrm{L}}(k,\omega)(\overline{\mathbf{I}} - \hat{k}\hat{k})}{\varepsilon^{\mathrm{L}}(k,\omega)\left(\varepsilon^{\mathrm{T}}(k,\omega) - n^2\right)}. \tag{A6}$$

Let us now evaluate the trace of the co-factor matrix. Noting the relations $\mathrm{tr}[\hat{k}\hat{k}] = 1, \mathrm{tr}[\overline{\mathbf{I}}] = 3$, the trace function $\gamma_l(\mathbf{k}) := \mathrm{tr}[\overline{\mathbf{C}}(\mathbf{k},\omega_l(\mathbf{k}))]$ from [1] applied to Eq. (A5) yields

$$\gamma_l(\mathbf{k}) := \left(\varepsilon^{\mathrm{T}}(k,\omega) - n^2\right)\left[\left(\varepsilon^{\mathrm{T}}(k,\omega) - n^2\right) + 2\varepsilon^{\mathrm{L}}(k,\omega)\right]. \tag{A7}$$

Next, in order to estimate the crucial $R_l(\mathbf{k})$ function

$$R_l(\mathbf{k}) = \left.\frac{\gamma_l(\mathbf{k})}{\omega\partial G^{-1}(\mathbf{k},\omega)/\partial\omega}\right|_{\omega=\omega_l(\mathbf{k})} \tag{A8}$$

constructed in [1], we use Eq. (A4) to compute

$$\frac{\partial G^{-1}(\mathbf{k},\omega)}{\partial\omega} = \frac{\partial\varepsilon^{\mathrm{L}}(k,\omega)}{\partial\omega}\left[\varepsilon^{\mathrm{T}}(k,\omega)-n^2\right]^2 + 2\varepsilon^{\mathrm{L}}(k,\omega)\left(\varepsilon^{\mathrm{T}}(k,\omega)-n^2\right)\frac{\partial\left(\varepsilon^{\mathrm{T}}(k,\omega)-n^2\right)}{\partial\omega}, \tag{A9}$$

which after substituting into Eq. (A8) and making use of Eq. (A7) results in the following expression

$$R_l(\mathbf{k}) := \left.\frac{\left(\varepsilon^{\mathrm{T}}(k,\omega)-n^2\right)+2\varepsilon^{\mathrm{L}}(k,\omega)}{\omega\dfrac{\partial\varepsilon^{\mathrm{L}}(k,\omega)}{\partial\omega}\left(\varepsilon^{\mathrm{T}}(k,\omega)-n^2\right)+2\omega\varepsilon^{\mathrm{L}}(k,\omega)\dfrac{\partial\left(\varepsilon^{\mathrm{T}}(k,\omega)-n^2\right)}{\partial\omega}}\right|_{\omega=\omega_l(\mathbf{k})} \tag{A10}$$

valid for arbitrary nonlocal isotropic and optically inactive metamaterials. Even though Eq. (A10) may still look complicated, it has the advantage that it does not require evaluating the modal field distribution functions $\hat{e}_l(\mathbf{k})$ and depends only on the dispersion relations $\omega_l(\mathbf{k})$ and the material tensor functions.

APPENDIX B. THE MOMENTUM-SPACE RADIATION FORMULA FOR GENERIC TIME-DOMAIN SOURCES

We convert the radiation formula (2) into a form more convenient for antenna applications involving arbitrary nonlocal metamaterial domains, i.e., not restricted to the isotropic media of Sec. 3. The direction of wave propagation is $\hat{k} := \mathbf{k}/k$, so we may describe this direction by a solid angle Ω. The magnitude $k = |\mathbf{k}|$ is related to frequency through the mode dispersion relation $\omega = \omega_l(k,\hat{k})$. It is better, however, to express the dispersion relation in the form

$$\frac{k^2c^2}{\omega^2} = n_l^2\left(\omega,\hat{k}\right), \tag{B1}$$

which is very frequently used in optics [5]. Here, n_l is the index of refraction of the lth mode and the positive square root of Eq. (B1) is assumed. The volume element $\mathrm{d}^3k/(2\pi)^3$ in momentum space can now be re-expressed in spherical coordinates, then we transform k to ω using Eq. (B1). Therefore,

$$\int_{\mathbb{R}^3}\frac{\mathrm{d}^3k}{(2\pi)^3} = \int_0^\infty \mathrm{d}\omega\int_{4\pi}\mathrm{d}\hat{k}\frac{\omega^2 n_l^2\left(\omega,\hat{k}\right)}{(2\pi c)^3}\frac{\partial}{\partial\omega}\left[\omega n_l\left(\omega,\hat{k}\right)\right]. \tag{B2}$$

We now introduce the antenna radiation pattern $U_l(\omega,\hat{k})$, which is defined by

$$\int_{\mathbb{R}^3}\frac{\mathrm{d}^3k}{(2\pi)^3}U_l(\mathbf{k}) = \int_0^\infty \mathrm{d}\omega\int_{4\pi}\mathrm{d}\hat{k}\;U_l\left(k,\hat{k}\right). \tag{B3}$$

Physically, $U_l(\omega,\hat{k})$ is the energy radiated in standard time interval with duration T per unit frequency per unit solid angle. Using Eqs. (B2) and (2), we finally arrive at

$$\boxed{U_l\left(\omega,\hat{k}\right) = \frac{\omega^2 n_l^2\left(\omega,\hat{k}\right)}{(2\pi c)^3}\frac{\partial}{\partial\omega}\left[\omega n_l\left(\omega,\hat{k}\right)\right]U_l\left[(\omega/c)n_l\left(\omega,\hat{k}\right)\hat{k}\right],} \tag{B4}$$

where

$$U_l\left[(\omega/c)n_l\left(\omega,\hat{k}\right)\hat{k}\right] = \mathbf{J}^*_{\mathbf{ant}}(\mathbf{k},\omega)\cdot\overline{\mathbf{R}}_l(\mathbf{k})\cdot\mathbf{J}_{\mathbf{ant}}(\mathbf{k},\omega)\big|_{\mathbf{k}=(\omega/c)n_l\left(\omega,\hat{k}\right)\hat{k}}. \tag{B5}$$

In writing Eqs. (B4) and (B5), we have used $\mathbf{k} = k\hat{k}$ then re-expressed k in terms of ω and $\hat{k}$ with the help of Eq. (B1). Consequently, the radiation mode antenna pattern intensity as function of direction and frequency is completely determined by the dispersion relation in Eq. (B1).

REFERENCES

1. Mikki, S., "Theory of electromagnetic radiation in nonlocal metamaterials: A momentum space approach — Part I (submitted)," *Progress In Electromagnetics Research B*, Vol. 89, 63–86, 2020.
2. Ginzburg, V. L., *The Propagation of Electromagnetic Waves in Plasmas*, Pergamon Press, Oxford, New York, 1970.
3. Landau, L. D., *Electrodynamics of Continuous Media*, Butterworth-Heinemann, Oxford, England, 1984.
4. Ginzburg, V. L., *Theoretical Physics and Astrophysics*, Pergamon Press, Oxford, New York, 1979.
5. Agranovich, V. and V. Ginzburg, *Crystal Optics with Spatial Dispersion, and Excitons*, Springer Berlin Heidelberg Imprint Springer, Berlin, Heidelberg, 1984.
6. Halevi, P., *Spatial Dispersion in Solids and Plasmas*, North-Holland, Amsterdam, New York, 1992.
7. Ilinskii, Y. A. and L. Keldysh, *Electromagnetic Response of Material Media*, Springer Science+Business Media, New York, 1994.
8. Sitenko, A. G., *Electromagnetic Fluctuations in Plasma*, Academic Press, 1967.
9. Fabrizio, M. and A. Morro, *Electromagnetism of Continuous Media: Mathematical Modelling and Applications*, Oxford University Press, Oxford, 2003.
10. Schelkunoff, S. A. and H. T. Friss, *Antennas: Theory and Practice*, Chapman & Hall, London, New York, 1952.
11. Balanis, C. A., *Antenna Theory: Analysis and Design*, 4th Edition, Inter-Science, Wiley, 2015.
12. Mikki, S. and A. Kishk, "Theory and applications of infinitesimal dipole models for computational electromagnetics," *IEEE Transactions on Antennas and Propagation*, Vol. 55, No. 5, 1325–1337, May 2007.
13. Mikki, S. and Y. Antar, "Near-field analysis of electromagnetic interactions in antenna arrays through equivalent dipole models," *IEEE Transactions on Antennas and Propagation*, Vol. 60, No. 3, 1381–1389, March 2012.
14. Clauzier, S., S. Mikki, and Y. Antar, "Generalized methodology for antenna design through optimal infinitesimal dipole model," *2015 International Conference on Electromagnetics in Advanced Applications (ICEAA)*, 1264–1267, September 2015.
15. Mikki, S. and Y. Antar, "On the fundamental relationship between the transmitting and receiving modes of general antenna systems: A new approach," *IEEE Antennas and Wireless Propagation Letters*, Vol. 11, 232–235, 2012.
16. Zeidler, E., *Quantum Field Theory II: Quantum Electrodynamics*, Springer, 2006.
17. Godement, R., *Analysis II: Differential and Integral Calculus, Fourier Series, Holomorphic Functions*, Springer-Verlag, Berlin, 2005.
18. Mikki, S. M. and A. A. Kishk, "Electromagnetic wave propagation in nonlocal media: Negative group velocity and beyond," *Progress In Electromagnetics Research B*, Vol. 14, 149–174, 2009.
19. Mikki, S. and Y. Antar, "On electromagnetic radiation in nonlocal environments: Steps toward a theory of near field engineering," *2015 9th European Conference on Antennas and Propagation (EuCAP)*, 1–5, April 2015.
20. Mikki, S. and Y. Antar, *New Foundations for Applied Electromagnetics: The Spatial Structure of Fields*, Artech House, London, 2016.
21. Mikki, S., "Exact derivation of the radiation law of antennas embedded into generic nonlocal metamaterials: A momentum-space approach," *2020 14th European Conference on Antennas and Propagation (EuCAP)*, 1–5, 2020.
22. Lathi, B. P. and Z. Ding, *Modern Digital and Analog Communication Systems*, Oxford University Press, New York, 2019.
23. Sarkar, D., S. Mikki, K. V. Srivastava, and Y. Antar, "Dynamics of antenna reactive energy using time-domain IDM method," *IEEE Transactions on Antennas and Propagation*, Vol. 67, No. 2, 1084–1093, Feb. 2019.
24. Schwinger, J., et al., *Classical Electrodynamics*, Perseus Books, Mass, 1998.